

Resonance Raman Studies on
Reaction Mechanism of Photolyases:
Structural Characteristics of the
Active Site and Photo-repair
Mechanism of UV-damaged DNA

Jiang Li

Doctor of Philosophy



Department of Photoscience

School of Advanced Sciences

The Graduate University for Advanced Studies
Japan

Prologue

Ultraviolet light irradiation induces formation of DNA dimer, which can lead to mutagenic processes. Cyclobutane pyrimidine dimer (CPD) and (6-4) photoproduct are the two major damages in DNA, which are repaired by CPD photolyase and (6-4) photolyase under blue light illumination, respectively.

Although structure and catalytic mechanism of CPD photolyase have been extensively studied, the unclear structure and environment of the active site in (6-4) photolyase needs to be clarified. (6-4) photolyases having neutral semiquinoid and oxidized forms of FAD were investigated by resonance Raman spectroscopy. DFT calculations on the neutral semiquinone were carried out for the first time. A special D₂O effect was recognized only after being oxidized once and photoreduced to form a semiquinone again, but not by simple H/D exchange of the solvent. The Raman spectral characteristics indicate strong H-bonding interactions, a fairly hydrophobic environment, and an electron-lacking feature in a benzene ring of the FAD cofactor, which seems to specifically control the reactivity of (6-4) photolyase.

The interaction between the active site and the damaged DNA in the both photolyases remains to be uncertain. Resonance Raman spectra of the complexes between damaged DNA and (6-4) or CPD photolyases in the neutral semiquinoid and oxidized forms were obtained. An interaction between UV-damaged DNA and the adenine ring of FAD was revealed in the both enzymes, while a direct interaction between UV-damaged DNA and the benzene ring of FAD was identified in CPD photolyase, but not in (6-4) photolyase. Such different interactions indicate that the two photolyases have different electron transfer mechanisms. Besides, alterations of H-bonding environment of FAD were observed upon substrate binding, which account for the reported higher redox potential of CPD photolyase, and may facilitate the reaction mechanism in the both enzymes.

List of Publications

1. Characteristic Structure and Environment in FAD Cofactor of (6-4) Photolyase along Function Revealed by Resonance Raman Spectroscopy, *Journal of Physical Chemistry B*, 2006 August 24th, 110(33): 16724-16732
2. Similarities and Differences between Cyclobutane Pyrimidine Dimer (CPD) Photolyase and (6-4) Photolyase as Revealed by Resonance Raman Spectroscopy: Electron Transfer Mechanism from FAD Cofactor to UV-Damaged DNA, *Journal of Biological Chemistry*, 2006 September 1st, 281(35): 25551-25559

Acknowledgements

I would like to express my deep and sincere gratitude to my supervisor Prof. Teizo Kitagawa from Okazaki Institute for Integrative Bioscience (OIIB) and Graduate University for Advanced Studies (SOKENDAI) for his valuable guidance and encouragement.

I am also deeply grateful to my advisor Dr. Takeshi Uchida (now in Hokkaido University) for his introduction to such an interesting field of Raman spectroscopy, stimulating suggestions and kind help.

I would like to express my gratitude to Dr. Takehiro Ohta for the valuable discussions about chemical calculations, and wish to express my sincere thanks to Prof. Takeshi Todo for his courtesy of providing the genes of photolyases. My warm thanks are due to all the other members of Kitagawa's Lab for their help, support, interest and valuable hints. Especially, I am obliged to Ms. Hiroko Mizuki for her help in preparing the enzyme.

Finally, I would like to give my special thanks to my wife Na Li whose patient love enabled me to complete this work.

June, 2006

Okazaki, Japan

Jiang Li

Contents

Prologue	ii
List of Publications	iii
Acknowledgements	iv
Contents	vii
List of Figures	x
List of Tables	xi
1 General Background	1
1.1 UV-damaged DNA and its Repair by Photoreactivation	1
1.2 Photolyase	3
1.2.1 Structure and Reaction Mechanism of CPD Photolyase . . .	3
1.2.2 (6-4) Photolyase	6
1.3 Resonance Raman Spectroscopy	7
1.4 Objective of This Study	8
2 Structure and Environment of FAD in (6-4) Photolyase	9
2.1 Abstract	9
2.2 Introduction	10
2.3 Experimental Methods	11
2.3.1 Enzyme Preparation	11
2.3.2 Enzyme Photoreduction	12
2.3.3 Enzyme Activity	12
2.3.4 Absorption and Resonance Raman Spectroscopy	12
2.3.5 Density Functional Theory Calculations	13
2.4 Results	13
2.4.1 Enzyme Activity of (6-4) Photolyase.	13
2.4.2 Absorption Spectra of (6-4) Photolyase	14

2.4.3	Resonance Raman Spectra of Semiquinoid (6-4) Photolyase .	15
2.4.4	Resonance Raman Spectra of Oxidized (6-4) Photolyase . . .	17
2.4.5	Density Functional Theory Calculation for Neutral Radical Semiquinoid Lumiflavin	20
2.5	Discussion	24
2.5.1	Comparison with CPD Photolyase	24
2.5.2	H-bonding Environment of FAD in (6-4) Photolyase	25
2.5.3	Hydrophobic Environment of FAD in (6-4) Photolyase	27
2.5.4	Low Electron Density of Ring I of FAD in (6-4) Photolyase .	27
2.5.5	Biological Implication	28
2.6	Conclusions	29
3	Interactions between UV-damaged DNA and FAD	30
3.1	Abstract	30
3.2	Introduction	31
3.3	Experimental Methods	34
3.3.1	Enzyme Preparation	34
3.3.2	Substrate Preparation	35
3.3.3	Enzyme Activity	35
3.3.4	Absorption and Resonance Raman Spectroscopy	35
3.4	Results	36
3.4.1	Enzyme Activity	36
3.4.2	Absorption Spectra of Photolyase Complexed with DNA Le- sions	37
3.4.3	Resonance Raman Spectra of Neutral Semiquinoid Photolyase Complexed with DNA Lesions	38
3.4.4	Resonance Raman Spectra of Oxidized Photolyase Com- plexed with DNA Lesions	40
3.5	Discussion	42
3.5.1	Interactions between UV-damaged DNA and the Isoallox- azine Ring of FAD	42
3.5.2	Interactions between UV-damaged DNA and the Adenine Ring of FAD	43
3.5.3	Alterations in Hydrogen Bonding Interactions around FAD Induced by Substrate Binding	45
3.5.4	Implication for Biological Functions	45
3.6	Conclusion	47

4	General Conclusion	48
4.1	Structural Characteristics of Active Site in Photolyases	48
4.1.1	FAD Cofactor	48
4.1.2	FAD Cofactor upon Substrate Binding	48
4.2	Implication for Photo-Repair Mechanism of UV-Damaged DNA . .	49
4.2.1	Similar Reaction Mechanisms in (6-4) and CPD Photolyases	49
4.2.2	Quantum Yield	49
4.2.3	Electron Transfer Pathway	50
	Bibliography	60
A	Supplementary Raman Spectra of CPD Photolyase	61
A.1	CPD Photolyase in D ₂ O	61
A.2	E109A Mutant without MTHF	62
B	Cartesian Coordinates for Optimized Lumiflavin	65
B.1	Neutral Semiquinoid Lumiflavin	65
B.2	Neutral Semiquinoid Lumiflavin with N3-D	66
B.3	Neutral Semiquinoid Lumiflavin with N3-D, N5-D	67

List of Figures

1.1	Structures of UV-damaged DNA. R: CH ₃ or H.	2
1.2	Illustration of photo-repair of UV-damaged DNA by photoreactivation.	2
1.3	Structures of flavin adenine dinucleotide (FAD) in different redox states.	3
1.4	Reaction mechanism of CPD photolyase.	4
1.5	Crystal structure of <i>E. coli</i> CPD photolyase (PDB ID: 1dnp).	5
1.6	Proposed mechanism for oxetane intermediate formation in (6-4) photolyase.	7
1.7	Illustration of Raman scattering.	7
2.1	Effect of illumination time on the extent of dimer repair by the His-tagged enzyme used in this experiment observed with damaged p(dT) ₈ . Absorbance at 266 nm (a) and that at 325 nm (b) of (6-4) photoproducts are plotted against time.	14
2.2	Absorption spectra of (6-4) photolyase from <i>Arabidopsis thaliana</i> (a) and the structure and atomic numbering scheme of flavin in three redox states (b-d). For (a) the solid line shows the spectrum of the enzyme immediately after purification, which is a mixture of a neutral semiquinoid form and an oxidized form, and the dashed line shows the photoreduced enzyme with a majority amount of the neutral semiquinoid form, while the dotted line shows that of the fully oxidized form. The arrows indicate the Raman excitation wavelengths. (b) oxidized form, (c) neutral semiquinoid form, (d) anionic fully reduced form.	15

- 2.3 Resonance Raman spectra of (6-4) photolyase from *Arabidopsis thaliana* which was photoreduced by blue light in H₂O (A), immediately after purification in H₂O (B) and in D₂O (C). Spectrum (D) was observed after 10 min in the repeated measurement in D₂O. Spectrum (E) were observed for the enzyme which was oxidized completely first and photoreduced subsequently by blue light in D₂O. The Raman excitation wavelength was 568.2 nm. 16
- 2.4 Resonance Raman spectra of oxidized (6-4) photolyase from *Arabidopsis thaliana* in H₂O (A) and D₂O (B) and those of free FAD in H₂O (C) and D₂O (D). The excitation wavelength was 488.0 nm. The FAD solution contains 4M KI to quench fluorescence. 19
- 2.5 Normal modes of some typical marker bands for neutral radical semiquinoid lumiflavin (A) and its corresponding N3-D/N5-D form (B). Vibrational frequencies and displacements were calculated by DFT method using Gaussian 03 with B3LYP/6-31G(d) basis functions. 22
- 2.6 Structure and sequence alignment for flavin center. (A) crystal structure of *E. coli* CPD photolyase. (B) Alignment of *E. coli* CPD photolyase, *Arabidopsis thaliana* (6-4) photolyase, and *Arabidopsis thaliana* cryptochrome 1 over the region in H-bonding distance from isoalloxazine 25
- 3.1 Structures of the UV-induced DNA lesions. R, H or CH₃. 31
- 3.2 Redox states and numbering scheme for the isoalloxazine ring of FAD in photolyase. 32
- 3.3 Structure of the FAD cofactor and a CPD-like DNA lesion in CPD photolyase (PDB ID: 1TEZ). The distances of possible interactions are given in Å. 33
- 3.4 Time course of absorption change of UV-damaged p(dT)₈ upon near-UV/visible light irradiation in the presence of (6-4) photolyase (A) and CPD photolyase (B). The absorbance at 266 nm (circles) is due to undamaged DNA, and that at 325 nm (triangles) is due to the (6-4) photoproduct. 36
- 3.5 Absorption spectra of (6-4) and CPD photolyases in the absence (solid line) and presence (dotted line) of UV-irradiated p(dT)₁₀. (A) Neutral semiquinoid (6-4) photolyase, (B) oxidized (6-4) photolyase, (C) neutral semiquinoid CPD photolyase, (D) oxidized CPD photolyase. The arrows indicate the Raman excitation wavelengths. 37

- 3.6 Resonance Raman spectra of 150 μM neutral semiquinoid (6-4) photolyase (A) and CPD photolyase (B). In both (A) and (B), subpanel (a) shows the spectrum for enzyme alone, (b) shows the spectrum in the presence of 300 μM p(dT)₁₀, (c) the spectrum in presence of 300 μM UV-irradiated p(dT)₁₀, (d) the difference spectrum [(b) - (a)] \times 3, and (e) the difference spectrum [(c) - (a)] \times 3. The Raman excitation wavelength was 568.2 nm. 38
- 3.7 Resonance Raman spectra of 75 μM oxidized (6-4) photolyase (A) and CPD photolyase (B). In both (A) and (B), subpanel (a) shows the spectrum for enzyme alone, (b) shows the spectrum in the presence of 150 μM p(dT)₁₀, (c) shows the presence of 150 μM UV-irradiated p(dT)₁₀, (d) the difference spectrum [(b) - (a)] \times 3, and (e) the difference spectrum [(c) - (a)] \times 3. The Raman excitation wavelength was 488.0 nm. G, Raman band of glycerol. Insert: Band X of (6-4) photolyase in the absence (solid line) and presence (dotted line) of UV-irradiated p(dT)₁₀. 40
- 3.8 Schematic illustration for the positions of a substrate and the putative electron transfer pathways in (6-4) photolyase (A) and CPD photolyase (B). (6-4)PP represents (6-4) photoproduct. 44
- A.1 Resonance Raman spectra of *E. coli* CPD photolyase in a semiquinoid form in D₂O (a), after 10 min repeated measurement in D₂O (b), and their difference spectrum (c). The Raman excitation wavelength was 568.2 nm. 62
- A.2 Absorption spectra of *E. coli* CPD photolyase in wide type (a) and E109A mutant (b). 63
- A.3 Resonance Raman spectra of *E. coli* CPD photolyase in a semiquinoid form as (a) wide type in H₂O, (b) E109A in H₂O, (c) wide type in D₂O, (d), E109A in D₂O. The Raman excitation wavelength was 568.2 nm. 64

List of Tables

2.1	Raman frequencies (cm^{-1}) of neutral radical semiquinoid flavins and flavoproteins	18
2.2	Assignments of Raman bands of neutral radical semiquinoid flavin in (6-4) photolyase	21
3.1	Raman frequency shifts (cm^{-1}) of FADH° in (6-4) photolyase and CPD photolyase upon substrate binding.	39
3.2	Raman frequency shifts (cm^{-1}) of FADH_{ox} in (6-4) photolyase and CPD photolyase upon substrate binding.	42

Chapter 1

General Background

1.1 UV-damaged DNA and its Repair by Photoreactivation

Ultraviolet light radiation in the wavelength range between 260 and 320 nm causes damage to DNA. Principally, such damage results from the dimerization of adjacent pyrimidines in the same DNA strand. This covalently linked dimer influences the replication and transcription, and leads to cell death or skin cancer [1]. Most (70-80%) of UV-induced DNA lesions is cyclobutane pyrimidine dimer (CPD) and, a lesser extent (20-30%) is (6-4) photoproduct as shown in Figure 1.1 [2].

There are some networks of repair mechanisms in most organisms to restore the UV-induced DNA damage and maintain genetic integrity. One of them is nucleotide excision repair, in which an oligonucleotide containing the lesion is excised from the DNA strand and the resulting single-strand gap refilled correspondingly. Another widespread mechanism by which dimers can be repaired is photo-repair (photoreactivation) [3]. In 1949, independent publications from Albert Kelner and Renato Dulbecco discovered the light-induced DNA repair [4]. After that, photolyase, a kind of enzyme with a flavin adenine dinucleotide (FAD) cofactor, was identified to catalyze the process of photoreactivation [5, 6, 7]. Compared with the complex multi-step processes of nucleotide excision repair, photoreactivation is a simpler and more direct way to provide a reliable reversion of pyrimidine dimers. Figure 1.2 illustrates the light-dependent process of enzymatic photoreactivation. That is, DNA photolyase binds to the UV-damaged DNA dimer and, upon absorbing a visible light photon (300-500 nm), splits DNA dimer, thus restoring the bases to their native forms.

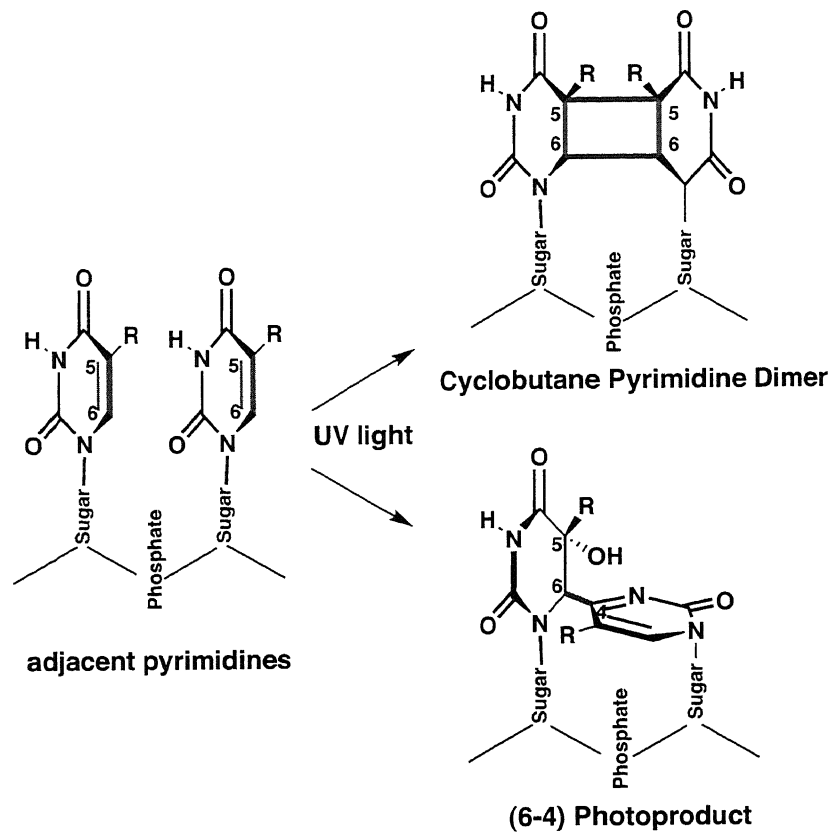


Figure 1.1: Structures of UV-damaged DNA. R: CH₃ or H.

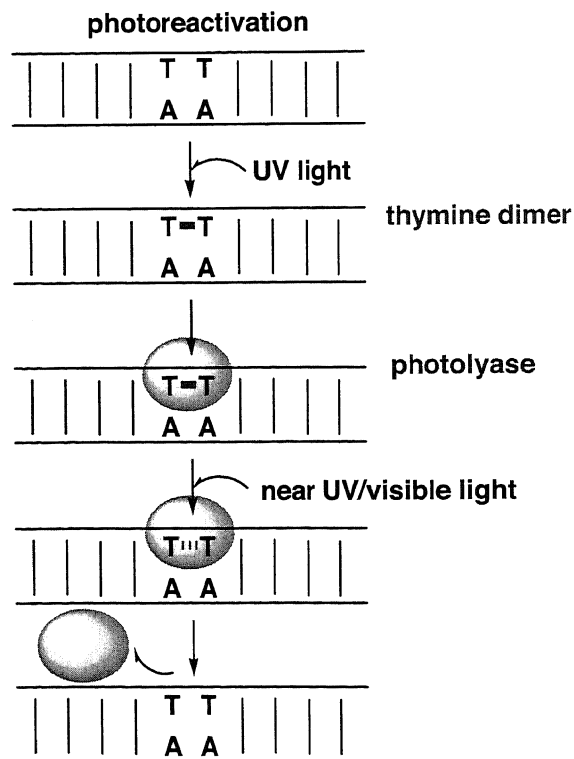


Figure 1.2: Illustration of photo-repair of UV-damaged DNA by photoreactivation.

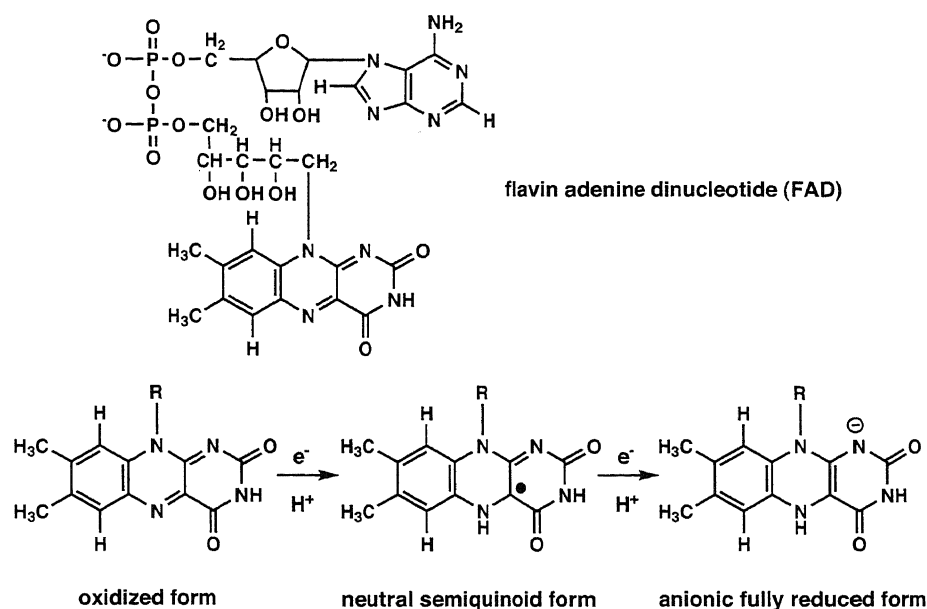


Figure 1.3: Structures of flavin adenine dinucleotide (FAD) in different redox states.

1.2 Photolyase

Photolyases are widespread in nature and have been reported in bacteria, plants, and animals. Corresponding to the UV-damaged DNA, there are two types of DNA photolyases. One specifically repairs CPD, the other repairs only (6-4) photoproduct. The former is called CPD photolyase and the latter (6-4) photolyase [2, 8]. The amino acid sequences of the two enzymes are similar to each other [9], although the chemical structures of their substrates are quite different.

Photolyase is a member of a DNA photolyase/blue light receptor protein family, which consists of three groups: CPD photolyase, (6-4) photolyase and blue light photoreceptor (cryptochrome, CRY). CPD photolyase is the best characterized and its reaction mechanism was elucidated in considerable detail. Compared with CPD photolyase, the structure and function of the other two groups have been less well studied.

1.2.1 Structure and Reaction Mechanism of CPD Photolyase

CPD photolyase contains FAD as an essential cofactor for DNA repairing. It is well known that flavin is a widespread chromophore in a biological system. This molecule has three different redox states; oxidized, semiquinoid and fully reduced forms. And such a diversity of redox state makes flavin a universal cofactor for electron transfer in many enzymes [10]. The structure and three possible redox states of the FAD cofactor in photolyase are shown in Figure 1.3. Only the anionic fully reduced form is the active state for enzymatic photoreactivation [11]. A sec-

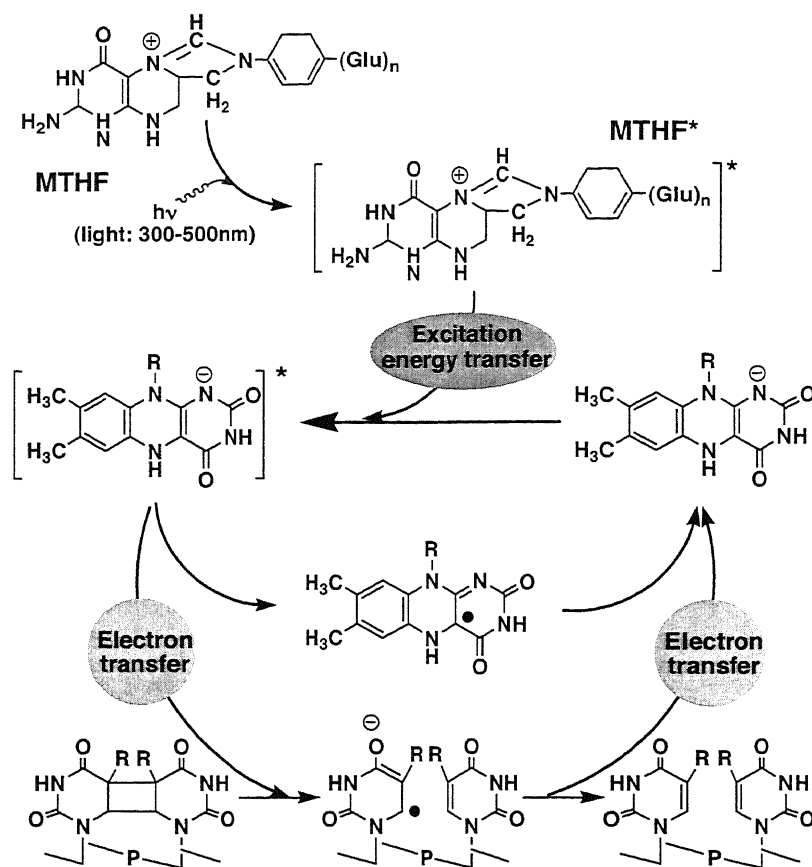


Figure 1.4: Reaction mechanism of CPD photolyase.

ond chromophore of either 5,10-methenyltetrahydrofolate polyglutamate (MTHF) [12] or flavin derivative [13] was discovered as an antenna to harvest the light in CPD photolyase.

The putative reaction mechanism of *E. coli* CPD photolyase was shown in Figure 1.4 [14]. Step 1: A blue light photon (350-450 nm) is absorbed by MTHF, or by anionic fully reduced FAD with a much lower efficiency due to its lower extinction coefficient. Step 2: The excited MTHF transfers energy to the anionic fully reduced FAD via dipole-dipole coupling between the donor and acceptor. Step 3: The excited anionic fully reduced FAD transfers an electron to CPD and changes to the neutral semiquinoid FAD concomitantly. Step 4: The C5-C5 and C6-C6 bonds of CPD (Figure 1.1) are cleaved by the electron from FAD. Step 5: Electron transfers back from the repaired DNA to the neutral semiquinoid FAD [8]. It is notable that the isolated CPD photolyase has a stable flavin radical in the neutral semiquinoid state because of the oxidation by oxygen in the air [15].

It has been found that the FAD cofactor in the inactive redox states (neutral semiquinoid or oxidized forms) undergoes a photoreduction by absorbing visible light to yield the catalytically active fully reduced form in photolyase. Several

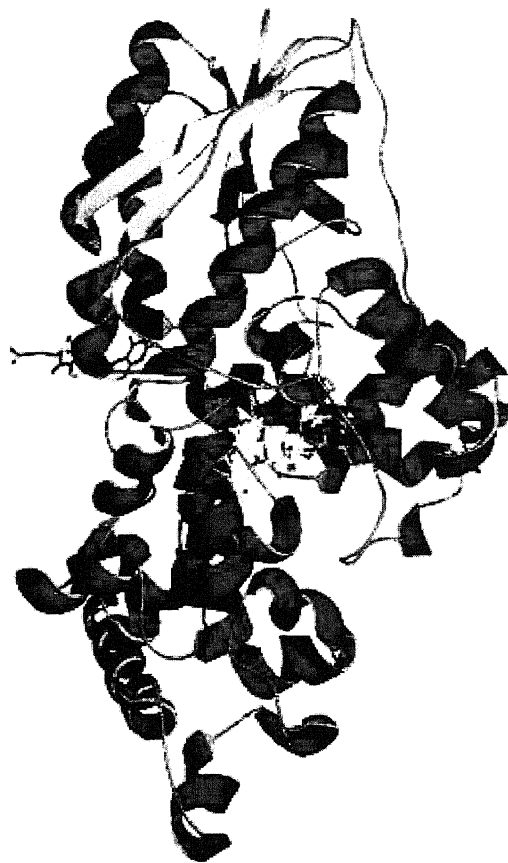


Figure 1.5: Crystal structure of *E. coli* CPD photolyase (PDB ID: 1dnp).

conserved tryptophans were identified to transfer an electron to the FAD cofactor during photoreduction [16, 17]. Besides, although it is generally assumed that back electron transfer from the repaired pyrimidine to the neutral semiquinoid FAD restores the cofactor before next catalytic cycle, the evidence for the Step 4 is still indirect. The strongest evidence for the supposed cyclic electron transfer as shown in Figure 1.4 is the finding that the quantum yield for photo-repair by the enzyme containing fully reduced FAD is 0.7-1.0, whereas the quantum field of photoreduction of neutral semiquinoid FAD to fully reduced FAD is only 0.05-0.1. Therefore, if photoreduction is necessary after each cycle of repair, the over all quantum yield of repair should be no more than that from photoreduction. So, the neutral semiquinoid FAD is not converted to fully reduced form in each cycle by photoreduction. Although a transient absorption study argued against the Step 4 that the FAD remains in the semiquinoid state after repairing and may be reduced to the fully reduced form by a different chemical source [18], a recent study of femtosecond spectroscopy supportes the catalytic photocycle [19].

Crystal structures of CPD photolyase have been resolved as shown in Figure 1.5 [20, 21, 22, 23]. This structure demonstrated that the FAD cofactor, which is located in a deeply buried pocket within a protein matrix and held by the

conserved residues through direct contacts, adopts an U-shaped conformation of isoalloxazine with an adenine ring in close proximity. Because all the reported FADs of flavoproteins in other protein family present an extended conformation, the unique U-shaped FAD is characteristic of DNA photolyase/blue light receptor protein family. It has been supposed that the U-shaped FAD (the adenine is stacked between isoalloxazine and UV-damaged DNA) facilitates electron transfer between isoalloxazine and substrate by effective coupling [24, 2, 25, 26].

A detailed structure of the enzyme-substrate complex is necessary to the thorough understanding of electron-transfer between the flavin cofactor and the DNA lesion. All the computational studies except one predicted a large distance of about 10 Å between the isoalloxazine ring and CPD [8]. Such a large distance was also supported by the experimental studies from EPR/ENDOR [24, 27]. However, the crystal structure of CPD photolyase complexed with a CPD-like DNA lesion shows a shorter distance (3-4 Å) that the substrate contacts both adenine and isoalloxazine of FAD [23]. The detailed structure of the active site containing substrate is uncertain until now.

1.2.2 (6-4) Photolyase

The anionic fully reduced FAD was also identified as the essential cofactor in (6-4) photolyase [28]. However, the second chromophore has not been isolated, and thus its existence is still uncertain. No crystal structure of (6-4) photolyase is available to date.

The genes for the (6-4) photolyase exhibit a sequence similarity to CPD photolyase, especially in the FAD binding sites [29]. Such high similarity indicates a similar structure and reaction mechanism in the two photolyases. Unlike CPD, a simple cleavage of the 6-4 C-C bond cannot restore the original forms of DNA from the (6-4) photoproduct. However, two conserved histidines in (6-4) photolyase have been identified to catalyze (6-4) photoproduct to form an oxetane intermediate by a thermal reaction when (6-4) photoproduct is bound to the enzyme (Figure 1.6) [30, 31]. Such an oxetane intermediate has a four-member ring, which is similar with CPD, and can be split by one incident electron [28]. Such finding confirms the close mechanistic similarities between (6-4) and CPD photolyases, which at first glance appear to catalyze different reactions.

Unexpectedly, (6-4) photolyase presents a much lower quantum yield (0.05-0.1) compared to that of CPD photolyase (0.7-1.0) [8]. This indicates the differences in structure and reaction mechanism between (6-4) and CPD photolyase. Such precise differences between CPD photolyase and (6-4) photolyase regarding substrate binding and DNA repair needs to be clarified.

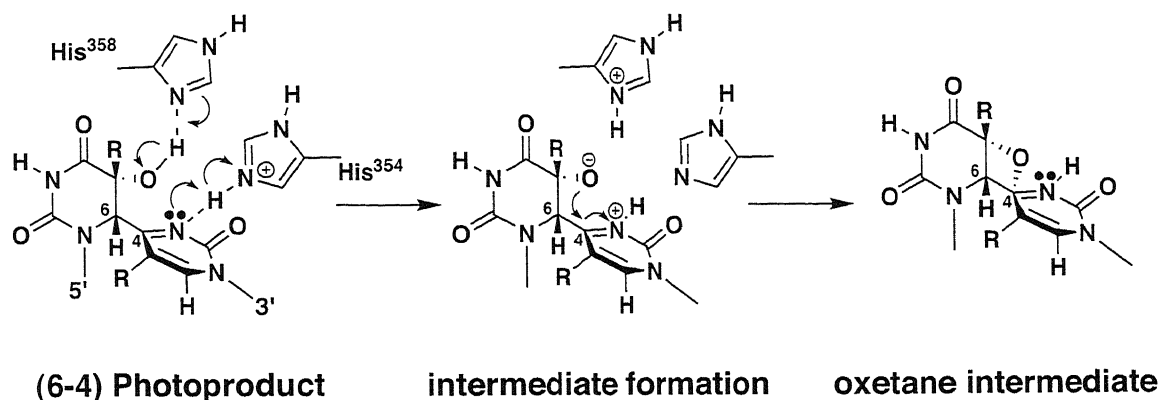


Figure 1.6: Proposed mechanism for oxetane intermediate formation in (6-4) photolyase.

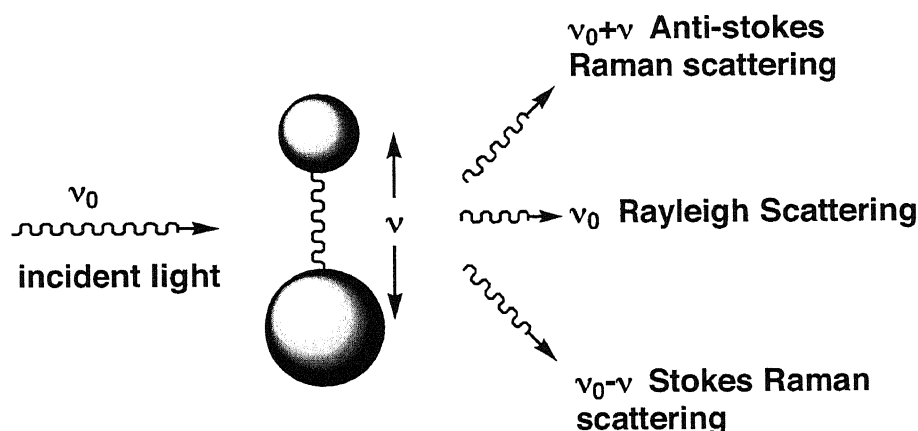


Figure 1.7: Illustration of Raman scattering.

Besides, (6-4) photolyase is also very similar with animal cryptochrome (CRY), another member of this protein family. For example, two genes having 41-45% sequence identity to *Drosophila* (6-4) photolyase are found in the human genome [9, 32, 33]. Thus, (6-4) photolyase is a bridge over two other groups in the protein family and the clarification of this enzyme may be helpful to provide implications for the understanding of the unclear CRY in human beings.

1.3 Resonance Raman Spectroscopy

As shown in Figure 1.7, the Raman scattering arises when a photon is incident on a molecule and interacts with the electric dipole of the molecule. It is a form of vibronic spectroscopy and the spectrum gives the vibrational frequencies of molecule. Therefore, the structure and environment of molecule can be revealed by its Raman spectra.

Resonance Raman effect occurs when the wavelength of the incident light is

close to that of the electronic absorption band of the molecule. The intensity of Raman scattering can be enhanced by 10^3 to 10^6 times. Because flavin is a chromophore with different intense absorption bands in different redox states, resonance Raman is a sensitive technique to probe the structure and environment of the flavin cofactor selectively without the influences from the protein matrix [34, 35].

Resonance Raman studies have been performed on neutral semiquinoid CPD photolyase and its complex with UV-damaged DNA [36, 37]. The low-frequency Raman bands indicate that the neutral semiquinoid FAD cofactor is in a strong hydrogen bonding environment. Further understanding of the detailed structure and environment of the FAD cofactor needs improved the current Raman assignments of neutral semiquinoid flavin.

1.4 Objective of This Study

This study investigated the structure of the active site along its functions in (6-4) and CPD photolyases by resonance Raman spectroscopy.

The precise structure of (6-4) photolyase is not clear until now. In Section 2, the electric structure and environment of the FAD cofactor in (6-4) photolyase was probed for the first time. First, the methods of expression, purification and evaluation of (6-4) photolyase were established and optimized. Then, resonance Raman spectra of the FAD cofactor in both oxidized and neutral semiquinoid forms were obtained. In order to enhance the understanding of the observed Raman spectra, DFT calculations were performed to improve the Raman assignments of neutral semiquinoid flavin. To clarify the detailed structure of the active site in (6-4) and CPD photolyases with substrate binding, the FAD cofactor in neutral semiquinoid and oxidized forms complexed with UV-damaged DNA in both enzymes were studied by resonance Raman spectroscopy in Section 3.

Chapter 2

Structure and Environment of FAD in (6-4) Photolyase¹

2.1 Abstract

A pyrimidine-pyrimidone (6-4) photoproduct and a cyclobutane pyrimidine dimer (CPD) are major DNA lesions induced by ultraviolet irradiation, and (6-4) photolyase, an enzyme with flavin adenine dinucleotide (FAD) as a cofactor, repairs the former specifically by light illumination. We investigated resonance Raman spectra of (6-4) photolyase from *Arabidopsis thaliana* having neutral semiquinoid and oxidized forms of FAD, which were selectively intensity enhanced by excitations at 568.2 and 488.0 nm, respectively. DFT calculations were carried out for the first time on the neutral semiquinone. The marker band of a neutral semiquinone at 1606 cm⁻¹ in H₂O, whose frequency is the lowest among various flavoenzymes, apparently splits into two comparable bands at 1594 and 1608 cm⁻¹ in D₂O, and similarly that at 1522 cm⁻¹ in H₂O does into three bands at 1456, 1508, and 1536 cm⁻¹ in D₂O. This D₂O effect was recognized only after being oxidized once and photoreduced to form a semiquinone again, but not by simple H/D exchange of solvent. Some Raman bands of the oxidized form were observed at significantly low frequencies (1621, 1576 cm⁻¹) and with band splittings (1508/1493, 1346/1320 cm⁻¹). These Raman spectral characteristics indicate strong H-bonding interactions (at N5-H, N1), a fairly hydrophobic environment, and an electron-lacking feature in benzene ring of the FAD cofactor, which seems to specifically control the reactivity of (6-4) photolyase.

¹J. Li, T. Uchida, T. Ohta, T. Todo, and T. Kitagawa, Characteristic Structure and Environment in FAD Cofactor of (6-4) Photolyase along Function Revealed by Resonance Raman Spectroscopy, *Journal of Physical Chemistry B*, 2006. This work was supported by Grants-in-Aid from the Ministry of Education, Culture, Sports, Science and Technology of Japan (MEXT) to T.K. (14001004). J. L. was supported by the scholarship from MEXT.

2.2 Introduction

Ultraviolet (UV) light irradiation to organisms causes damages of cellular DNA by forming a dimer between adjacent pyrimidine bases, which can result in mutation, cell death, and cancer afterward [1]. Most of the damaged DNA are cyclobutane pyrimidine dimer (CPD) and (6-4) photoproduct, which are repaired by CPD photolyase and (6-4) photolyase, respectively, under illumination by near-UV/visible light [38, 39].

For CPD photolyase, structure and mechanism of the enzymatic reaction have been extensively studied. The resting CPD photolyase contains an anionic fully reduced FAD (FADH^-) as an essential cofactor and also either 5,10-methenyltetrahydrofolate polyglutamate (MTHF) or flavin derivative as a light-harvesting chromophore [8]. Crystal structures of CPD photolyase have demonstrated that the FAD cofactor, which is located in a deeply buried pocket within a protein matrix and held by the conserved residues through direct contacts, adopts an unusual and unique U-shaped conformation of isoalloxazine with an adenine ring in close proximity [20, 21, 22, 23]. The latest crystal structure of CPD photolyase complexed with a CPD-like DNA lesion shows that the adenine ring of FAD bridges the electron donating isoalloxazine ring and the electron accepting substrate [23]. The proposed repair mechanism of CPD photolyase is as follows: after recognizing and binding to CPD, the light-harvesting chromophore or FADH^- absorbs a photon, and then, its excited state, FADH^{-*} is formed either directly or by energy transfer from a light-harvesting chromophore. Next, FADH^{-*} transfers an electron to the CPD, which splits it into two pyrimidine monomers, and then FADH^{-*} is converted into a neutral semiquinoid form (FADH°). Finally, an electron is transferred back from the repaired DNA to FADH° to restore the FADH^- [8]. Transient absorption studies, however, argued against the last stage of the mechanism that the FAD remains in the semiquinoid state after repair and may be reduced to FADH^- by a different chemical source [18].

Since the amino acid sequence of (6-4) photolyase, especially in the FAD binding domain, is similar to that of CPD photolyase, it has been proposed that these two enzymes share a similar structure and reaction scheme [29, 9, 40, 41, 30]. However, no crystal structure has been available for (6-4) photolyase, and therefore, its reaction mechanism is not well understood [2]. It has been noted that (6-4) photolyase has a significantly lower quantum yield (0.05-0.1) of DNA repair compared with that of the CPD enzyme (0.7-0.98) [8], and the reason for this remains to be explained.

For a flavin to perform a specific enzymatic reaction, control of its redox potential by a protein is indispensable [10]. To explore the structure of the FAD

cofactor and its environment in (6-4) photolyase, we measured resonance Raman spectra of the FAD cofactor in both the neutral semiquinoid and oxidized forms, since resonance Raman spectroscopy is a sensitive tool to probe the structure of flavin and its interactions with the protein environment [34, 35]. Normal mode assignments of Raman bands for the neutral semiquinoid flavin were performed for the first time using density functional theory (DFT) calculations on lumiflavin at the B3LYP/6-31G(d) level. Our results suggest that the FAD of (6-4) photolyase has a structure in which electron density is lacking in the benzene ring and strong hydrogen bonds are formed at N5-H and N1 in an overall hydrophobic environment, and its relationship to functions will be discussed.

2.3 Experimental Methods

2.3.1 Enzyme Preparation

The gene of (6-4) photolyase from *Arabidopsis thaliana* [42] was inserted at the *NdeI/SacI* sites of the pET-28a expression vector (Novagen). *Escherichia coli* BL21(DE3) transformed with the vector was inoculated into 0.5 L of culture in a 3-L flask and grown at 37°C in LB medium to OD₆₀₀ of 1.5 and then cooled to 26°C. IPTG was added to 0.2 mM. The culture was further incubated for about 24 hours and then harvested. After harvest, the pellet was frozen at -80°C, thawed, and resuspended in a lysis buffer (20 mM sodium phosphate, 0.5 M NaCl, 1 mM DTT, 5% glycerol, pH 7.4). Following the sonication, the cell debris was removed by ultracentrifugation. The cell-free extract was loaded onto a HisTrap HP column (Amersham), and the fusion protein was eluted with the elution buffer (20 mM sodium phosphate, 0.5 M NaCl, 0.5 M imidazole, pH 7.4). Then, the sample was applied to a HiTrap Heparin HP column (Amersham) and eluted with a linear gradient of NaCl from 0.3 M to 1 M. The sample was identified as a monomeric form by a HiLoad 16/60 Superdex 200 prep grade column (Amersham). Starting from 2 L of the *E. coli* culture, ca. 12 mg of the purified protein was obtained after the Heparin column.

The purified enzyme was stored in 20 mM sodium phosphate (pH 7.4) containing 0.5 M NaCl. Purity of the protein after the Heparin column was determined by SDS-PAGE, and the molecular weight of the monomeric enzyme was confirmed with the gel filtration method under the assumption that the elution volume of the Superdex 200 column was the same as that scaled by Gel Filtration Calibration Kit (Amersham). The concentration of the oxidized form of the enzyme was estimated on the basis of the FAD absorbance at 450 nm ($\epsilon_{450} = 1.12 \times 10^4 \text{ M}^{-1} \text{ cm}^{-1}$) [43], and that of the neutral semiquinoid form was estimated from the absorbance

at 580 nm ($\epsilon_{580} = 4.8 \times 10^3 \text{ M}^{-1}\text{cm}^{-1}$) [44].

2.3.2 Enzyme Photoreduction

(6-4) photolyase as purified is composed of semiquinoid FAD and oxidized FAD. All the semiquinoid enzymes in this mixture were completely oxidized by air in 48 hours because of its sensitivity to oxygen. To prepare the semiquinoid form, the oxidized enzyme was photoreduced by laser irradiation at 442 nm from a He-Cd laser (Kimmon Electric, IK4101R-F). First, 100 μL of the solution containing 150 μM (6-4) photolyase was placed in a cylindrical Raman cell and sealed with a rubber septum. Then, the inside of the cell was replaced with N_2 , and the cell was spun at a rate of 2,000 rpm. The laser light was focused onto the sample evenly with a quartz lens of 150-mm focal length to increase the efficiency of photoreduction. To avoid the cell heating by laser illumination, the spinning cell was cooled by flushing with cold N_2 gas passed through liquid N_2 . About 30 min illumination with 30 mW laser light was sufficient to reduce 150 μM (6-4) photolyase. Reduction of a majority of the oxidized FAD to the semiquinoid form was confirmed with absorption spectra.

2.3.3 Enzyme Activity

The method for measuring the enzyme activity of (6-4) photolyase was based on the procedure established for CPD photolyase [45]. A substrate of the damaged DNA was prepared through irradiation of $\text{p}(\text{dT})_8$ by 254 nm UV-light from a UV transilluminator (Vilber Lourmat, TFX-20-MC), with 6.4 mW/cm^2 of intensity for 30 min using the cylindrical spinning cell cooled by cold N_2 . The complex of 2 μM (6-4) photolyase with 50 μM damaged $\text{p}(\text{dT})_8$ in 50 mM Tris-HCl (pH 7.4), 200 mM NaCl, and 1 mM DTT was illuminated by tungsten light (Sigma Koki, PHL-150) at room temperature. The UV-vis absorption spectrum of the reacting sample in the spinning cell was measured with the intervals of 1-min.

2.3.4 Absorption and Resonance Raman Spectroscopy

Optical absorption spectra of samples were recorded with a Hitachi UV-3310 UV-vis spectrophotometer at room temperature. Resonance Raman spectra were obtained with a single monochromator (Jobin Yvon, SPEX750M) equipped with a liquid N_2 -cooled CCD detector (Roper Scientific, Spec10:400B/LN). The excitation wavelengths used were 568.2 nm and 488.0 nm from a krypton-argon mixed gas ion laser (Spectra Physics, BeamLok 2060) for the semiquinoid and oxidized forms, respectively. The laser power at the sample point was 5 mW. Rayleigh

scattering was removed with appropriate holographic notch filters (Kaiser Optical Systems). Raman shifts were calibrated with indene, and the accuracy of the peak positions of the well-defined Raman bands was $\pm 1 \text{ cm}^{-1}$.

An aliquot of the $150 \mu\text{M}$ enzyme solution in 20 mM sodium phosphate buffer at pH 7.4 containing 0.5 M NaCl was used for the measurement of the semiquinoid form, while the $80 \mu\text{M}$ enzyme or isolated FAD solution in the same buffer was used for the measurements of the oxidized enzyme or isolated FAD. All the measurements were performed with a spinning Raman cell containing $100 \mu\text{L}$ of the sample solution, and the semiquinoid samples were purged with N_2 to avoid the oxidation. All samples were cooled with cold N_2 gas. The structureless background in the final spectrum was removed by a polynomial subtraction procedure by Igor Pro 5.03 (WaveMetrics).

2.3.5 Density Functional Theory Calculations

To analyze the Raman bands of the FAD neutral semiquinoid form, geometry optimizations and frequency calculations were carried out for a model compound, lumiflavin, in its neutral radical semiquinoid form by the DFT method on the B3LYP/6-31G(d) level. To see the deuterated effect of flavin on calculated normal modes and those frequencies, the H atom bound at the N3 and N5 positions was replaced with the D atom. The structures with the minimal energy were confirmed by the absence of imaginary frequencies. The obtained frequencies were scaled by the widely accepted single scaling factor of 0.9614 [46]. All calculations were carried out on an SGI2800 high performance computer (Research Center for Computational Science, Okazaki) using the program package Gaussian 03 [47].

2.4 Results

2.4.1 Enzyme Activity of (6-4) Photolyase.

Figure 2.1 shows the time course of dimer repair observed with $2 \mu\text{M}$ (6-4) photolyase and $50 \mu\text{M}$ damaged $\text{p}(\text{dT})_8$ in the reaction buffer as described in the Experimental Methods. For the damaged DNA, the 266 nm band of normal DNA is decreased significantly and a band at 325 nm of the (6-4) photoproducts [48] is appreciable. Along the illumination of white light for the damaged DNA in the presence of (6-4) photolyase, reappearance of the band at 266 nm (a) and disappearance of the band at 325 nm (b) were observed, while no change was observed in the absence of the enzyme (data not shown), demonstrating that the His-tagged enzyme used in this study is activity like a GST-tagged enzyme [42].

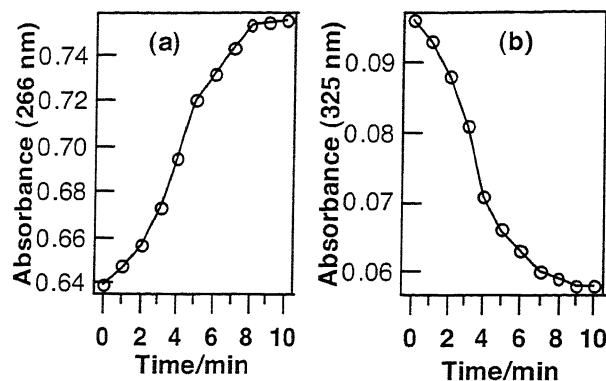


Figure 2.1: Effect of illumination time on the extent of dimer repair by the His-tagged enzyme used in this experiment observed with damaged $p(dT)_8$. Absorbance at 266 nm (a) and that at 325 nm (b) of (6-4) photoproducts are plotted against time.

2.4.2 Absorption Spectra of (6-4) Photolyase

The three redox states including oxidized (FAD_{ox}), semiquinoid ($FADH^\circ$), and fully reduced ($FADH^-$) forms, are possible for an isoalloxazine ring, and their structures and atomic numbering are illustrated in Figure 2.2(b-d). Immediately after purification, the enzyme was a mixture of FAD_{ox} and $FADH^\circ$ as shown by a solid line in Figure 2.2(a). The fully oxidized form, which is shown by a dotted line in Figure 2.2(a), was obtained by exposure of the above mixture to air for 48 hours. The absorption spectrum of the fully oxidized (6-4) photolyase is remarkably different from that of FAD in a polar solvent, while it is similar to that in a nonpolar solvent [49]. The similarity of absorption spectra suggests that FAD in (6-4) photolyase is bound in a less polar environment.

The semiquinoid form was obtained by reduction of the oxidized enzyme by irradiation of blue light as explained in the Experimental Methods, which gave an absorption spectrum as the dashed line in Figure 2.2(a). The absorption maxima at 589 and 635 nm of a solid and dashed line in Figure 2.2(a) are due to the $\pi \rightarrow \pi^*$ electronic transition of $FADH^\circ$, while they are completely absent in the spectra of FAD_{ox} and $FADH^-$ (data not shown). On account of these absorption spectra, 568.2 nm was chosen as the Raman excitation wavelength to selectively enhance the neutral semiquinoid form, while 488.0 nm was chosen to enhance the pure oxidized form.

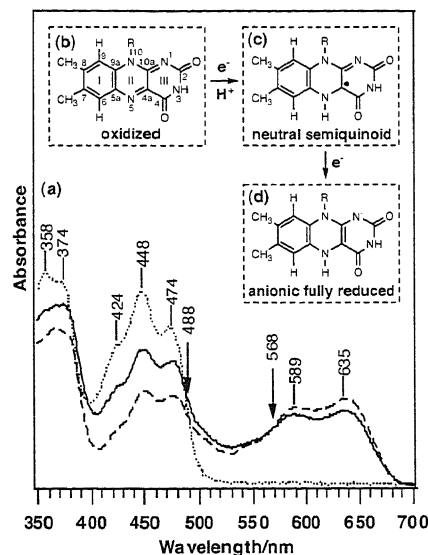


Figure 2.2: Absorption spectra of (6-4) photolyase from *Arabidopsis thaliana* (a) and the structure and atomic numbering scheme of flavin in three redox states (b-d). For (a) the solid line shows the spectrum of the enzyme immediately after purification, which is a mixture of a neutral semiquinoid form and an oxidized form, and the dashed line shows the photoreduced enzyme with a majority amount of the neutral semiquinoid form, while the dotted line shows that of the fully oxidized form. The arrows indicate the Raman excitation wavelengths. (b) oxidized form, (c) neutral semiquinoid form, (d) anionic fully reduced form.

2.4.3 Resonance Raman Spectra of Semiquinoid (6-4) Photolyase

The resonance Raman spectra of the photoreduced form in H_2O is shown in Figure 2.3 (A). The prominent bands in the H_2O solution at 1606, 1522, 1398, 1298, and 1220 cm^{-1} correspond well to bands of riboflavin neutral semiquinoid radical generated by pulse radiolysis at 1617, 1542, 1387, 1296, and 1225 cm^{-1} , which are Raman spectroscopically distinct from those of anion and cation radicals [50]. Therefore, Figure 2.3(A) demonstrates the formation of a neutral semiquinone (Figure 2.2c) in (6-4) photolyase. The spectrum B in Figure 2.3 is of the enzyme immediately after purification. Although the enzyme contains some amount of the oxidized form as shown in Figure 2.2(a), the observed Raman spectrum (Figure 2.3B) is almost identical to that of the photoreduced form (Figure 2.3A), since the bands are solely ascribed to the semiquinoid form due to the advantage of resonance effect of Raman excitation at 568.2 nm.

Spectrum (C) was observed for the sample whose solvent was replaced with D_2O immediately after purification of the enzyme in H_2O . Spectrum (C) is different from spectrum (B) with regard to the bands at 1341, 1323, and 1227 cm^{-1} , indicating that deuteration occurred. However, prolonged measurements brought

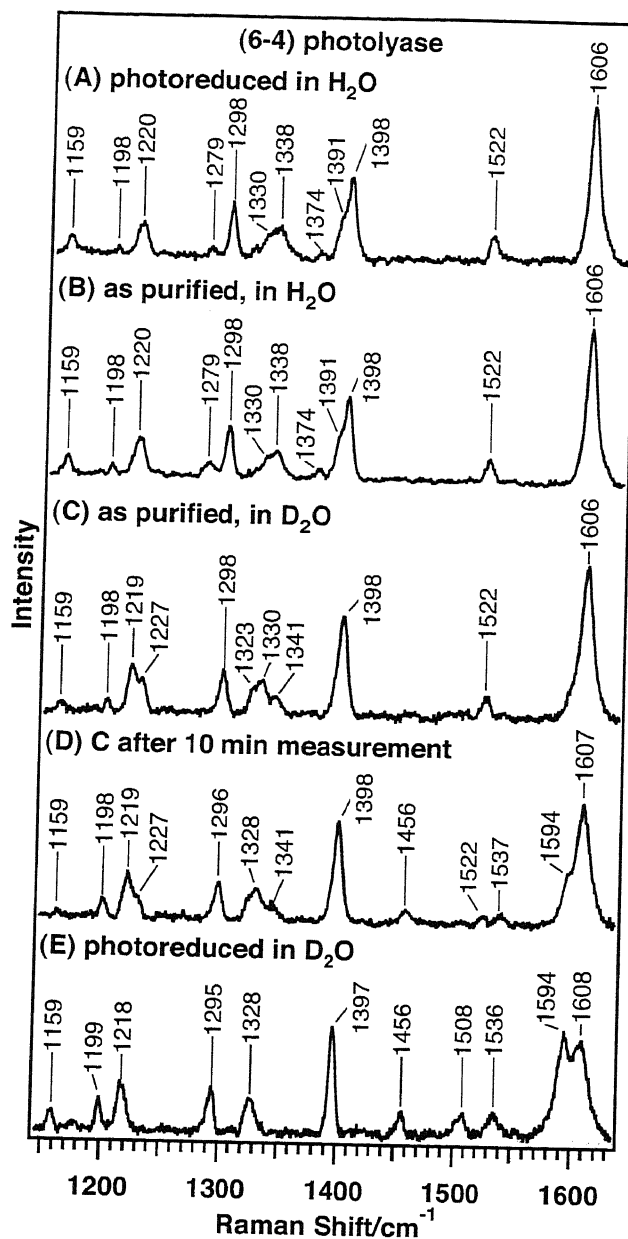


Figure 2.3: Resonance Raman spectra of (6-4) photolyase from *Arabidopsis thaliana* which was photoreduced by blue light in H₂O (A), immediately after purification in H₂O (B) and in D₂O (C). Spectrum (D) was observed after 10 min in the repeated measurement in D₂O. Spectrum (E) were observed for the enzyme which was oxidized completely first and photoreduced subsequently by blue light in D₂O. The Raman excitation wavelength was 568.2 nm.

about further changes. After 10 min of measurements, for example, the bands at 1522 and 1606 cm^{-1} seemed to split into three and two bands, respectively, as illustrated in spectrum (D). The sample of (E) was obtained separately by photoreduction in D_2O after complete oxidation of the purified enzyme in air. Because the proton attached at N5 of the semiquinoid flavin is released from the nitrogen atom in the oxidized form (Figure 2.2b), the above processes of oxidation and subsequent photoreduction in D_2O lead complete replacement of the H atom at N5 with the D atom. Accordingly, the spectral change in spectrum (D) compared with spectrum (C) seems to reflect the progress of N5-deuteration of FAD through photoreduction by the probe light along measuring time. Since spectrum (C) is different from either spectrum (B) in H_2O or spectrum (E) of the fully N5-D form, it is considered to reflect the N3-D form. It means that spectra (C) and (E) correspond to the N3-D/N5-H and N3-D/N5-D forms of isoalloxazine, respectively. Accordingly, the bands at 1594, 1536, 1508, and 1456 cm^{-1} are characteristic of N5-D, while those around 1200-1350 cm^{-1} are mainly due to N3-D.

Raman bands of the FADH° of (6-4) photolyase are listed in Table 2.1 and are compared with those of other flavins and flavoproteins in a neutral radical form [36, 37, 51, 52, 53, 50].

It is noted that the frequencies of prominent Raman bands of (6-4) photolyase are close to those of CPD photolyase. No Raman bands have been found so far in the 1400-1500 cm^{-1} region for the neutral semiquinoid flavins [50]. For (6-4) photolyase in the N5-D form, however, a band was observed at 1456 cm^{-1} for the first time. The reported Raman studies on CPD photolyase have not discussed the bands in this region because of the interference by the bands of Hepes [36] or glycerol [37] in the solvent. We can avoid this problem by using 20 mM phosphate buffer without glycerol. Vibrational assignment of these bands will be described quantitatively later on the basis of DFT calculations.

2.4.4 Resonance Raman Spectra of Oxidized (6-4) Photolyase

Figure 2.4 shows the resonance Raman spectra of the oxidized (6-4) photolyase in H_2O (A) and D_2O (B).

The vibrational assignment of the oxidized flavin has been well established [55, 54, 56, 57] and the customary numbering of Raman bands is given in the upper part of the figure. Band I of the oxidized flavin, which is attributed to an almost pure Ring I mode and is generally observed around 1630 cm^{-1} [51, 55, 57, 58, 59, 60, 61, 62, 63, 64, 65, 66], appeared at a distinctly lower frequency for (6-4) photolyase (1621 cm^{-1} in both H_2O and D_2O). All bands above 1340 cm^{-1} are $\text{H}_2\text{O}/\text{D}_2\text{O}$ insensitive, meaning that they arise from Rings I and/or II since neither

Table 2.1: Raman frequencies (cm^{-1}) of neutral radical semiquinoid flavins and flavoproteins

compound	solvent	Raman bands															Ref.
		1606	1594	1522	1508	1456	1398	1374	1338	1330	1298	1279	1220	1198	1225		
(6-4) Photolyase, FADH°	H ₂ O	1606		1522			1398	1374	1338	1330		1298	1279	1220	1198	[36]	
(6-4) Photolyase, FADH°	D ₂ O	1608	1594	1536	1508	1456	1397			1328		1295		1218	1199	this work	
CPD Photolyase, FADH°	H ₂ O	1607		1529			1392	1378	1347	1332		1303	1260	1222	1198	[36]	
CPD Photolyase, FADH°	D ₂ O	1607	1593	1529	1508		1392	1378		1332	1325	1302	1260	1222		[36]	
CPD Photolyase, FADH°	H ₂ O	1606		1528			1391			1332		1301		1220		[37]	
CPD Photolyase, FADH°	D ₂ O	1606	1594	1528			1390	1377		1332	1322	1300		1219		[37]	
P-450 Reductase, FADH°	H ₂ O	1611		1540			1378					1305	1264	1226		[51]	
P-450 Reductase, FMNH°	H ₂ O	1611		1532			1388					1304	1268	1227	1200	[51]	
Adrenodoxin, FADH°	H ₂ O	1611							1344			1310	1271			[52]	
Flavodoxin, FMNH°	H ₂ O	1611	1535				1378	1333	1314		1308	1269	1232		[51, 53]		
Fd, FMNH°	D ₂ O	1611				1386									[53]		
riboflavin (RF), RPH°	H ₂ O	1617		1542			1387					1296		1225		[50]	

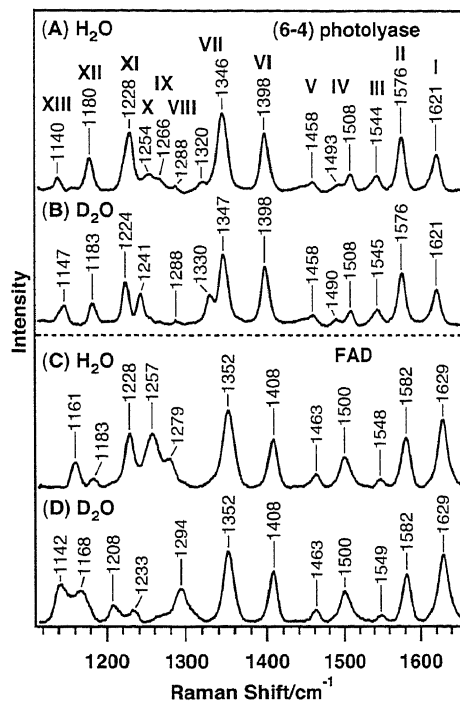


Figure 2.4: Resonance Raman spectra of oxidized (6-4) photolyase from *Arabidopsis thaliana* in H₂O (A) and D₂O (B) and those of free FAD in H₂O (C) and D₂O (D). The excitation wavelength was 488.0 nm. The FAD solution contains 4M KI to quench fluorescence. Band numbering is according Ref. [54].

ring has exchangeable protons. However, the bands at 1254, 1266 and 1320 cm⁻¹ in H₂O were shifted to lower or higher frequencies in D₂O (1241 and 1330 cm⁻¹). These are characteristic of the C2-N3 and N3-C4 stretching modes coupled with the N3-H bending mode, which exhibits a higher frequency shift upon removal of the coupling with N-H bending vibration in the N3-D form [59], but is shifted to lower by the coupling with the N3-D bending vibration.

Since the Raman spectrum of the oxidized CPD photolyase has not been reported yet, the spectra of the protein-free FAD in H₂O (C) and D₂O (D), measured under the same experimental condition except for addition of 4 M KI to quench the fluorescence, are presented for comparison in the lower part of Figure 2.4. The bands above 1350 cm⁻¹ are generally insensitive to the H/D substitution, in agreement with the results of (6-4) photolyase. The bands of free FAD in H₂O in the 1150-1300 cm⁻¹ region are shifted in D₂O in a complicated way, reflecting the participation of the N3-H bending vibration. The differences in these frequencies between (6-4) photolyase and free FAD are caused by differences in H-bonding at N3-H with the protein in water.

From the comparison of Rings I and II modes between (6-4) photolyase and free FAD, it is noticed that frequencies are generally lower and the intensity of the band at 1621 cm⁻¹ (band I) is weaker for protein than for free FAD. Since

band II is known to exhibit downshifts upon formation of a hydrogen bond at N1 [57], its lower frequency suggests that a strong hydrogen bond is formed at N1 of FAD in (6-4) photolyase. Splittings of band IV (1508 and 1493 cm^{-1}) and band VII (1346 and 1320 cm^{-1}) of the oxidized (6-4) photolyase are used as a marker of “buried” character of the flavin environment [55]. In fact, both bands are observed as a single band for free FAD (spectrum C), while it is split in a solid state [55]. Therefore, this observation indicates that the isoalloxazine ring of (6-4) photolyase is held in a well-formed protein pocket from which water molecules might be excluded. In addition, it is noted that the downshifted and weakened band I (1621 cm^{-1}), intensified band III (1544 cm^{-1}), downshifted band VI (1398 cm^{-1}), downshifted and weakened band IX (1266 cm^{-1}), weakened band X (1254 cm^{-1}), downshifted and intensified band XII (1180 cm^{-1}), and weakened band XIII (1140 cm^{-1}), all resemble the spectral characteristics of flavin placed in a less polar solvent [61, 67].

2.4.5 Density Functional Theory Calculation for Neutral Radical Semiquinoid Lumiflavin

Since there has been no theoretical treatment of vibrational spectra of neutral semiquinone of flavin, we carried out DFT calculations on lumiflavin at B3LYP/6-31G(d) level, and the results are summarized in Table 2.2, where the frequencies observed for (6-4) photolyase in H_2O and D_2O are compared with those calculated (scaled by a factor of 0.9614) [46] for the N3-H/N5-H, N3-D/N5-H, and N3-D/N5-D forms. In addition, included are the mode numbers and the approximate descriptions for vibrational character. Calculated vibrational modes are also illustrated in Figure 2.5, where the displacements of atoms are explicitly represented [68]. Cartesian coordinates of atoms in the minimal potentials obtained are given in Appendix B. The mode numbers are assigned tentatively in the order of increasing frequency, although the numbering is not established yet. Tentative assignments of the Raman bands observed for FADH° in (6-4) photolyase are also contained.

According to this calculation, the prominent band at 1606 cm^{-1} in H_2O can be assigned to an overlapped band of ν_{75} and ν_{74} , which include Ring I and primarily Ring II vibrations, respectively. ν_{75} does not shift upon N5-H deuteration, while ν_{74} downshifts by 7 cm^{-1} due to fairly large involvement of N5-H bending motion in the ν_{74} mode. Therefore, they are observed as separate bands in D_2O .

The alteration of resonance Raman band in the 1400-1550 cm^{-1} region upon deuterium substitution exhibits complex behavior. The 1522 cm^{-1} band observed in H_2O seems to split into 1536, 1508, and 1456 cm^{-1} in D_2O , as judged from

Table 2.2: Assignments of Raman bands of neutral radical semiquinoid flavin in (6-4) photolyase

observed (6-4) photolyase		calculated frequencies for lumiflavin					approximate descriptions
H ₂ O	D ₂ O	mode	N3-H N5-H ν/cm^{-1}	N3-D N5-H $\Delta\nu/\text{cm}^{-1}$	N3-D N5-D		
1606	1606	ν_{75}	1602	-1	-1	$\nu(\text{Ring I})$	
	1594	ν_{74}	1591	0	-7	$\nu(\text{Ring I}), \delta(\text{N}_5\text{-H}), \nu(\text{N}_1=\text{C}_{10a}), \nu(\text{C}_{4a}\text{-N}_5)$	
	1536	ν_{73}	1539	0	0	$\nu(\text{Ring I}), \nu(\text{N}_1=\text{C}_{10a})$	
1522	1508	ν_{72}	1503	0	-2	$\nu(\text{Ring I}), \delta(\text{N}_5\text{-H})$	
	1456	ν_{71}	1495	-1	-46	$\delta(\text{N}_5\text{-H}), \nu_{asym}(\text{C}_{4a}\text{-N}_5\text{-C}_{5a}), \nu(\text{N}_1=\text{C}_{10a})$	
1398	1397	ν_{61}	1398	0	-2	$\nu(\text{Ring I}), \nu(\text{N}_1=\text{C}_{10a}), \nu(\text{C}_{4a}\text{-N}_5), \nu_{asym}(\text{C}_{9a}\text{-N}_{10}\text{-C}_{10a})$	
1338	1328	ν_{59}	1345	-4	-19	$\delta(\text{N}_5\text{-H}), \delta(\text{N}_3\text{-H}), \nu_{sym}(\text{C}_{9a}\text{-N}_{10}\text{-C}_{10a}), \nu_{sym}(\text{C}_{10a}\text{-N}_1\text{-C}_2), \nu_{asym}(\text{N}_3\text{-C}_4\text{-C}_{4a})$	
1330		ν_{58}	1335	-124	-170	$\delta(\text{N}_3\text{-H}), \delta(\text{N}_5\text{-H})$	
1298	1298	ν_{57}	1312	-1	-5	$\nu(\text{Ring I}), \nu_{sym}(\text{C}_{9a}\text{-N}_{10}\text{-C}_{10a}), \delta(\text{N}_5\text{-H})$	
1279		ν_{56}	1298	+5	+2	$\nu(\text{Ring I}), \nu_{asym}(\text{C}_{9a}\text{-N}_{10}\text{-C}_{10a}), \delta(\text{N}_3\text{-H}), \delta(\text{N}_5\text{-H})$	

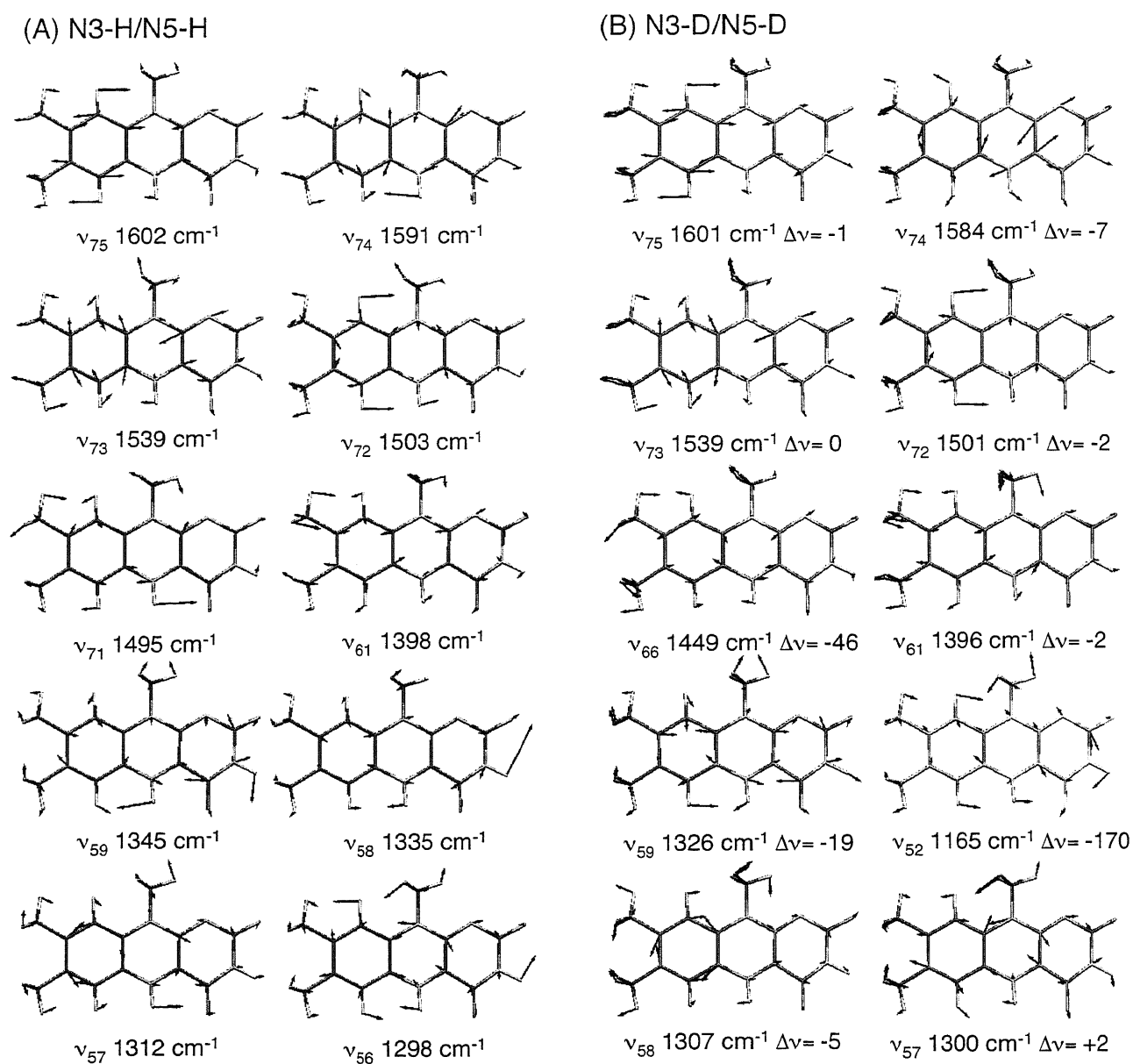


Figure 2.5: Normal modes of some typical marker bands for neutral radical semiquinoid lumiflavin (A) and its corresponding N3-D/N5-D form (B). Vibrational frequencies and displacements were calculated by DFT method using Gaussian 03 with B3LYP/6-31G(d) basis functions.

concomitant intensity decrease of the 1522 cm^{-1} band and intensity increase of those three bands. These bands were presumably assigned to the three computed normal modes, ν_{73} , ν_{72} , and ν_{71} , in the $1500\text{-}1540\text{ cm}^{-1}$ region. Upon deuteration the normal coordinate compositions are altered for the vibrational modes in this region, and thereby resonance Raman intensity redistribution, which are interpreted below. The ν_{73} mode is mainly composed of the $\text{N1}=\text{C10a}$ stretching and Ring I symmetric modes, and is expected to get strong resonance Raman enhancement due to a large change in polarizability along those symmetric modes. Furthermore, appreciable excited state distortion of the $\text{N1}=\text{C10a}$ bond is expected upon the $\pi \rightarrow \pi^*$ excitation at 568.2 nm , and it would cause redistribution of electron density regarding the $\text{N1}=\text{C10a}$ bond. The ν_{73} mode does not include vibration arising from N-H motion, and thus does not show large change in both the frequency and the normal mode in the deuterated form. The ν_{72} mode mainly consists of C-H bending in Ring I and N-H bending which is coupled weakly with the Ring I mode. Upon deuteration, the coupling of the N-H motion is removed, showing slight downshift in the frequency. The ν_{72} mode in the H-form may not be strongly resonance enhanced due to the C-H bending character of the vibrational mode. However, upon deuteration, the ν_{72} normal mode compositions are slightly altered. As mentioned above, the coupling with N-H bending is removed, and the mixing of the $\text{N1}=\text{C10a}$ stretching mode could cause resonance enhancement of Raman intensity. The ν_{71} mode at 1495 cm^{-1} is mainly composed of N5-H bending, to which $\text{N1}=\text{C10a}$ stretching and the asymmetric C4a-N5-C5a stretching [$\nu_{asym}(\text{C4a-N5-C5a})$] that can be intensity enhanced by the $\pi \rightarrow \pi^*$ excitation are coupled. This mode should show a large deuterium isotope shift, and the corresponding mode in the deuterium substituted form could be found as the ν_{66} mode at 1449 cm^{-1} . Thus, the 1456 cm^{-1} band observed in D_2O would arise from the ν_{66} mode. In the H_2O form, however, the ν_{66} mode is mainly composed of C-H bending motion of the methyl substituents of Ring I, which would not gain resonance Raman enhancement. When N5 is deuterated, ν_{66} contains the $\text{N1}=\text{C10a}$ and C4a-N5 stretchings and accordingly gains Raman intensity.

The intense band of Figure 2.3(A) at 1398 cm^{-1} is assignable to ν_{61} , which involves $\text{N1}=\text{C10a}$ and C4a-N5 stretching. Therefore, its frequency would be insensitive to deuterium exchange as observed both theoretically and experimentally. The shoulder peak at 1391 cm^{-1} and the nearby weak band at 1374 cm^{-1} disappear in D_2O . A couple of bands around 1338 cm^{-1} probably arise from ν_{59} and ν_{58} . The ν_{58} mode is almost pure N3-H and N5-H deformational mode, which exhibits a large downshift in the frequency upon deuteration. The bands of Figure 2.3(A) at 1298 and 1279 cm^{-1} are probably assigned to ν_{57} and ν_{56} , respectively.

2.5 Discussion

2.5.1 Comparison with CPD Photolyase

The marker band of the neutral semiquinoid flavin [69] for (6-4) photolyase was observed at 1606 cm^{-1} (Figure 2.3A), which is similar to that observed for CPD photolyase at 1607 [36] or 1606 [37] cm^{-1} (Table 1). These frequencies are lower than those of other flavins and flavoproteins [50, 37, 36, 69, 52, 51, 53, 70]. However, this marker band at 1606 cm^{-1} in (6-4) photolyase in H_2O splits into two comparable bands at 1608 and 1594 cm^{-1} in D_2O (Figure 2.3E), whereas that of CPD photolyase in D_2O remains a single band with a shoulder at 1593 cm^{-1} , which is very similar to that of (6-4) photolyase obtained after prolonged measurement in Figure 2.3(D). Figure 2.3(D) is inferred to arise from the incompletely N5-deuterated sample, because for (6-4) photolyase the redox cycle in this study (oxidation and subsequent photoreduction in D_2O) enforced the release of the N5 proton of flavin and replaces it with deuterium in a D_2O solvent, which gives the spectrum of the completely N5-deuterated sample as observed in Figure 2.3 (E). Consequently, it is highly likely that the reported spectrum of CPD photolyase in D_2O [37, 36] reflects an incompletely N5-deuterated enzyme. The assignment from DFT calculations that ν_{74} is low-frequency shifted but ν_{75} is invariable in the N5-D form (Table 2) also supports that the deuterium exchange at N5 causes its apparent splitting.

Another H/D sensitive band at 1522 cm^{-1} in H_2O splits into three bands at 1456 , 1508 , and 1536 cm^{-1} in D_2O . The split band at 1508 cm^{-1} was observed for CPD photolyase in one report [36] but not in the other [37], while the split band at 1456 cm^{-1} has not been observed in flavoproteins before. This apparent splitting is actually a frequency separation of accidentally degenerate bands due to a low-frequency shift of ν_{72} and ν_{71} in D_2O , while the higher-frequency counterpart (ν_{73}) is less sensitive to N5 deuteration. Although the corresponding Raman band of CPD photolyase at 1528 [37] or 1529 [36] cm^{-1} had no H/D effect, a similar H/D-sensitive resonance Raman band in this region was also observed for *Clostridium Mp.* Flavodoxin [53].

A prominent H/D-insensitive band was observed at 1398 cm^{-1} (with a shoulder at 1391 cm^{-1}) and a nearby H/D-sensitive band at 1374 cm^{-1} . The corresponding bands in CPD photolyase were observed at 1392 and 1378 cm^{-1} , respectively. Schelvis et al. proposed that the band at 1378 cm^{-1} in CPD photolyase might be a marker for the MTHF or its structural role by stabilizing the protein environment of the FAD cofactor [36], because this band was not observed for the MTHF-free mutant of CPD photolyase [37]. Since the purified (6-4) photolyase in this study

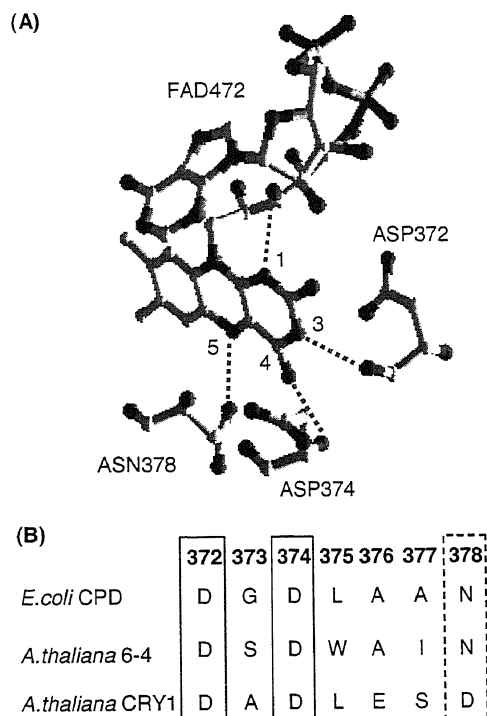


Figure 2.6: Structure and sequence alignment for flavin center. (A) crystal structure of *E. coli* CPD photolyase. (B) Alignment of *E. coli* CPD photolyase, *Arabidopsis thaliana* (6-4) photolyase, and *Arabidopsis thaliana* cryptochrome 1 over the region in H-bonding distance from isoalloxazine (from Refs. [20, 42, 71]).

does not contain the second chromophore, the 1374 cm^{-1} band cannot be ascribed to the MTHF moiety. Our theoretical assignment suggests that the intense band at 1398 cm^{-1} arises from the ν_{61} mode. Since ν_{61} involves N1=C10a and Ring II stretching characters, its strong resonance Raman intensity is reasonable. The weak band at 1374 cm^{-1} probably arises from Ring III of FAD in H_2O but is shifted to lower frequencies upon N3 deuteration.

2.5.2 H-bonding Environment of FAD in (6-4) Photolyase

The crystal structure of *E. coli* CPD photolyase revealed the H-bonding environment of FAD as illustrated in Figure 2.6. Hydrogen bonds are formed at N1, N3-H, C4=O and N5-H in CPD photolyase. The 2'-OH of the ribityl chain forms a hydrogen bond with N1 probably because of the unusual U-shaped FAD structure. N3-H donates a hydrogen bond to Asp372 (numbering in *E. coli* CPD photolyase), C4=O accepts a hydrogen bond from Asp374, and N5-H donates a hydrogen bond to Asn378. These amino acids involving hydrogen bonds are conserved in (6-4) photolyase. A very similar U-shaped FAD and H-bonding environment were also observed for the structure of the photolyase-like domain of cryptochrome 1 from *Arabidopsis thaliana*, except that the Asn378, which is contacted with N5-H, is

replaced by Asp [71]. A sequence alignment in this region is illustrated in Figure 2.6 (B). From the sequence alignment and resonance Raman spectra of (6-4) photolyase, the presence of similar hydrogen bonds at N5-H and N1 in (6-4) photolyase is indicated as discussed below.

We have already pointed out that the 1606 cm^{-1} marker band is assignable to an overlapped band of ν_{74} and ν_{75} . Its significantly lower frequency is a common feature to photolyases: 1607 cm^{-1} for CPD photolyase and 1606 cm^{-1} for (6-4) photolyase. Murgida et al. attributed the origin of the unusually low frequency of this band to a stronger hydrogen bond at N5-H [37], although Schelvis et al. argued against it, because its frequency is rather insensitive to H/D exchange. However, as mentioned above, deuteration in the sample of Schelvis et al. was probably incomplete, and presumably, N5-H was not replaced with deuterium. In this study, splitting of this marker band into two comparable components at 1608 and 1594 cm^{-1} was observed for the completely deuterated FAD cofactor in Figure 2.3 (E). The normal modes of ν_{74} assigned for 1594 cm^{-1} band involve N5-H bending deformations (Table 2, Figure 2.5), which will downshift upon H-bonding at N5-H as discussed by Murgida et al. before [37]. Therefore, the unusually low frequency of this marker band would indicate a strong hydrogen bond at N5-H in both the photolyases. Similarly, the lower frequencies of the 1522 cm^{-1} band in (6-4) photolyase and 1529 cm^{-1} band in CPD photolyase, which are presumably assigned to the modes of ν_{73} - ν_{71} with N5-H bending in ν_{72} and ν_{71} , also indicate a strong hydrogen bond at N5-H. This band was empirically used as an indicator of a hydrogen bond at N5-H in the Raman study on P-450 reductase [51], and it is justified by this study. Furthermore, judging from the lower frequencies of 1606 and 1522 cm^{-1} in (6-4) photolyase, the N5-H hydrogen bond would be much stronger in (6-4) photolyase than that in CPD photolyase.

As mentioned above, band II of the oxidized (6-4) photolyase indicates a strong hydrogen bond at N1. This hydrogen bond would be caused by the U-shaped FAD conformation as shown in Figure 2.6. The proteins in this family are believed to be characterized as the unique U-shaped FAD in which an adenine ring approaches the isoalloxazine ring near the N10-C10a moiety, whose stretching significantly contributes to the ν_{61} mode of the semiquinoid form (Table 2). Therefore, the ring stacking geometry may affect the ν_{61} Raman frequency and intensity and may cause the appearance of a weak sideband at 1391 cm^{-1} in Figure 2.3(A). The coupled bands around 1338 cm^{-1} , which involve N3-H and N5-H bending, have a different frequency (1325 cm^{-1}) and profile from that in CPD photolyase which may indicate different H-bonding environments between these two enzymes. On all accounts, the hydrogen bonds predicted for (6-4) photolyase are similar to those of CPD photolyase and cryptochrome except a stronger interaction at N5-

H, indicating a similar H-bonding environment of the flavin moiety in the DNA photolyases and blue light photoreceptor family.

2.5.3 Hydrophobic Environment of FAD in (6-4) Photolyase

Resonance Raman and UV-vis absorption spectra of the oxidized FAD in (6-4) photolyase are similar to those of the isolated flavin in a nonpolar solvent. Furthermore, Raman marker bands of “buried” flavin are also observed for (6-4) photolyase. This evidence indicates that the FAD cofactor in (6-4) photolyase is placed in a hydrophobic and less polar environment, as identified for CPD photolyase [72, 73]. Spiro’s model of flavin, supported by resonance Raman [67] and NMR [74] investigations, argued that the isoalloxazine ring prefers a zwitterionic resonance form in a polar solvent, which results in a higher frequency of band I for the oxidized flavin [54]. According to this model, the observed lower frequency of band I for (6-4) photolyase means a decreased polarity in a flavin pocket.

The hydrophobic environment around FAD of (6-4) photolyase was also suggested by the insensitivity of N5-H to the H/D exchange. To exchange the labile proton with solvent, water molecules must access to the exchange site. The strong hydrophobic environment in the active site of photolyase limits the approach of solvent water to N5 of the flavin ring, which also leads to difficulty in the exchange of N5-H. This coincides with the unexpected finding that N5-H deuteration proceeds little for CPD photolyase as well as (6-4) photolyase.

2.5.4 Low Electron Density of Ring I of FAD in (6-4) Photolyase

Previous work has shown that the C8-Cl substitution of a riboflavin binding protein exhibits a downshift of band I of the oxidized flavin Ring I mode from 1631 cm^{-1} to 1624 cm^{-1} and weakened it greatly [75]. It is believed that the C8-Cl substitution reduces the electron density of Ring I due to the electron withdrawing effect of chloride. Therefore, a significantly low-frequency and weak Raman intensity of band I (1621 cm^{-1}) observed for the oxidized (6-4) photolyase (Figure 2.4A) suggests that Ring I of the oxidized FAD lacks electrons.

The prominent band at 1398 cm^{-1} of FADH° in (6-4) photolyase has a higher frequency than those of other flavins and flavoproteins. This is assignable to ν_{61} , which is an out-of-phase mode of the N1=C10-C4a-N5 stretching and accordingly sensitive to the radical character (Table 2, Figure 2.5). This assignment is consistent with the intensity loss of the corresponding 1391 cm^{-1} band in CPD photolyase reconstituted with 1,3,5,10- ^{15}N -FAD [37]. Thus, its high frequency of

1398 cm^{-1} for (6-4) photolyase and 1391-1392 cm^{-1} for CPD photolyase may mean the higher radical density in the N1=C10a-C4a-N5 moiety. This is consistent with theoretical and EPR studies which pointed out that FADH° has a more localized radical spin density in CPD photolyase than in other flavoproteins and a very low electron density on Ring I [73, 24]. This trend is slightly stronger in (6-4) photolyase than in CPD photolyase.

One of the controlling factors of the electron density of flavin is an electrostatic effect [10]. In this family of proteins, two aspartic acids (Asp372 and Asp374, numbering in *E. coli* CPD photolyase) near Ring III are conserved. These negatively charged groups would readily induce an electronic perturbation to the ring system, especially to suppress the negative charge of Ring III in the resonance form. Thus, the electrostatic effect from the Asp residues may contribute to keep the flavin in photolyases in the neutral form and to make an electron density of Ring I low.

2.5.5 Biological Implication

H-bonding environment is an important factor to control the redox states of flavin in flavoproteins [10]. In the study on the control of redox potentials in flavodoxin from Ludwig et al., the G57T mutant, whose hydrogen bond at N5-H of flavin is expected to be weaker evaluated by crystal structure and $\text{p}K_a$ of N5-H, has a significantly increased redox potential for the semiquinone/hydroquinone couple [76]. Therefore an increased H-bonding interaction at N5-H may decrease the redox potential of semiquinoid flavin and make its reduction less favorable. In photolyases, FADH° is generated during repair and must be reduced to FADH^- before the next catalytic cycle. As for CPD photolyase, the FADH° was believed to be reduced by an electron from the repaired DNA, because the quantum yield of this enzyme is almost 1 [8]. In our study, (6-4) photolyase has a similar protein environment of FAD cofactor compared with that of CPD photolyase except for a stronger hydrogen bond at N5-H. Therefore, this stronger hydrogen bond may decrease the redox potential of FADH° and make its reduction reaction before next repair cycle difficult. If the FADH° in (6-4) photolyase is not reduced by repaired DNA but reduced by photoreduction from another photon, the significantly low quantum yield for this enzyme compared with CPD photolyase can be explained.

The hydrophobic and less polar environment, with small reorganization energy, will slow the back electron transfer from substrate radical to neutral semiquinoid FAD before repairing and therefore would be advantageous to electron transfer in the repairing process as pointed out for CPD photolyase [73, 77]. Such a scheme will also satisfy the repairing process of (6-4) photolyase, in which a hydrophobic environment of FAD cofactor was revealed.

Although the crystal structures of CPD photolyase showed that Ring I is in the direction of the DNA lesion [20, 21, 22, 23], the low spin density and possible low whole electron density on Ring I implies that electron transfer between isoalloxazine ring and CPD would not be direct [2, 24]. It was assumed that the adenine of the U-shaped FAD bridges the gap and provides effective coupling between isoalloxazine and damaged DNA [25, 26]. On the other hand, the recent study with femtosecond absorption spectroscopy concluded a direct electron jump from the FAD to the CPD, because the intramolecular electron transfer could not be observed without substrate [19]. In (6-4) photolyase, however, a FAD cofactor with more localized spin density and moderately low electron density of Ring I was observed, suggesting a higher possibility of an indirect electron transfer.

2.6 Conclusions

The resonance Raman spectra of neutral semiquinoid and oxidized forms of (6-4) photolyase were reported and interpreted with DFT calculations for the first time. The DFT calculations gave a theoretical basis for the behavior of some marker bands in relation with the environment around FAD. It is demonstrated that N5-H of the FAD cofactor of (6-4) photolyase is in a hydrophobic interior and has strong H-bonding interactions with the protein, which explains its peculiar behavior in the H/D exchange as well as the low quantum yield. The unique character of Raman spectra of the oxidized form can also be interpreted in terms of electrostatic and H-bonding interactions of FAD with protein residues conserved in this family of proteins. Implications from this study will be also helpful to understand a mechanism of blue light sensor proteins such as cryptochrome 1.

Chapter 3

Interactions between UV-damaged DNA and FAD¹

3.1 Abstract

Cyclobutane pyrimidine dimer (CPD) and (6-4) photoproduct, two major types of DNA damage caused by ultraviolet (UV) light, are repaired under illumination with near-UV/visible light by CPD photolyase and (6-4) photolyase, respectively. To understand the mechanism of DNA repair, we examined the resonance Raman spectra of complexes between damaged DNA and the neutral semiquinoid and oxidized forms of (6-4) and CPD photolyases. The marker band for a neutral semiquinoid flavin and band I of the oxidized flavin, which are derived from the vibrations of the benzene ring of FAD, were shifted to lower frequencies upon binding of damaged DNA by CPD photolyase but not by (6-4) photolyase, indicating that CPD interacts with the benzene ring of FAD directly but that (6-4) photoproduct does not. Bands II and VII of the oxidized flavin and the 1398/1391 cm^{-1} bands of the neutral semiquinoid flavin, which may reflect the bending of the U-shaped FAD, were altered upon substrate binding, suggesting that CPD and (6-4) photoproduct interact with the adenine ring of FAD. When substrate is bound, there is an upshifted 1528 cm^{-1} band of the neutral semiquinoid flavin in CPD photolyase, indicating a weakened hydrogen bond at N5-H of FAD, and in (6-4) photolyase, band X seems to be downshifted, indicating a weakened hydrogen bond at N3-H of FAD. These Raman spectra led us to conclude that the two photolyases have different electron transfer mechanisms as well as different

¹Jiang Li, Takeshi Uchida, Takeshi Todo, Teizo Kitagawa. Similarities and Differences between Cyclobutane Pyrimidine Dimer (CPD) Photolyase and (6-4) Photolyase as Revealed by Resonance Raman Spectroscopy: Electron Transfer Mechanism from FAD Cofactor to UV-damaged DNA, *Journal of Biological Chemistry*, 2006. This work was supported by Grants-in-Aid from the Ministry of Education, Culture, Sports, Science and Technology of Japan (MEXT) to T.K. (14001004). J. L. was supported by a scholarship from MEXT.

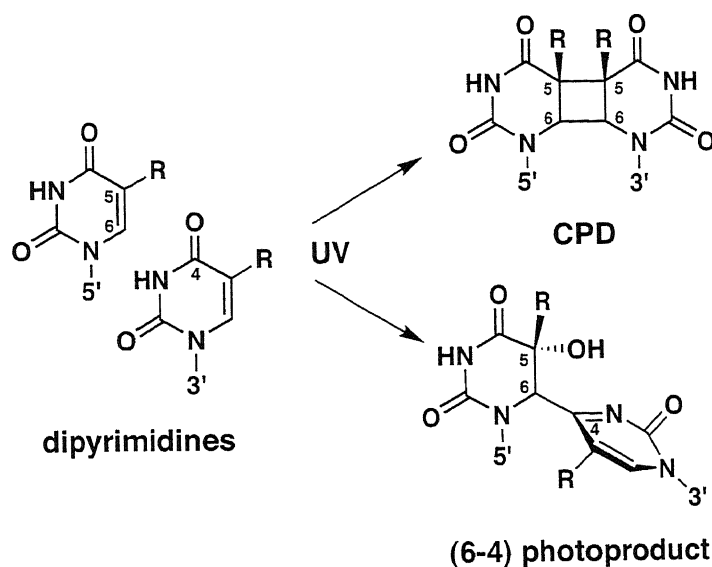


Figure 3.1: Structures of the UV-induced DNA lesions. R, H or CH₃.

hydrogen bonding environments, which account for the higher redox potential of CPD photolyase.

3.2 Introduction

Irradiation of organisms with ultraviolet (UV)² light causes damage to cellular DNA by inducing dimer formation between adjacent pyrimidine bases. This DNA damage causes mutation, cell death, and can lead to cancer [1]. Cyclobutane pyrimidine dimer (CPD) and (6-4) photoproduct (Figure 3.1) account for most of this DNA damage, and these are repaired by CPD photolyase and (6-4) photolyase, respectively, under illumination by near-UV/visible light [38, 39]. Similar association constants of ca. 10^{-9} M were identified for CPD and (6-4) photoproduct in the complex of corresponding photolyase, respectively, whereas those for the undamaged DNA is more than four orders of magnitude lower or not detectable [8, 40, 78]. Both photolyases contain flavin adenine dinucleotide (FAD) as an essential catalytic cofactor [79, 28]. The amino acid sequences of (6-4) and CPD photolyases, especially within the FAD binding region, are closely related, suggesting that these two enzymes share similar structure and reaction mechanisms [9]; however, the quantum yield for photorecovery is significantly lower for (6-4) photolyase than for CPD photolyase [8, 78, 30].

The isoalloxazine ring of FAD in a photolyase can exist in one of three possible

²The abbreviations used are: UV, ultraviolet; FAD, flavin adenine dinucleotide; FADH^o, neutral semiquinoid FAD; FADH⁻, anionic fully reduced FAD; FAD_{ox}, oxidized FAD; FMN, flavin mononucleotide; CPD, cyclobutane pyrimidine dimer; EPR, electron paramagnetic resonance; ENDOR, electron-nuclear double resonance; LUMO, lowest unoccupied molecular orbital.

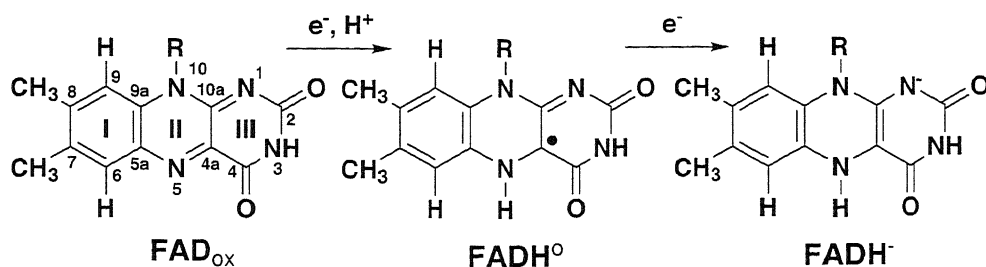


Figure 3.2: Redox states and numbering scheme for the isoalloxazine ring of FAD in photolyase.

states: oxidized (FAD_{ox}), neutral semiquinoid (FADH°), and anionic fully reduced (FADH^-) forms (Figure 3.2). FADH^- is considered to be the active form of flavin in photolyase. The first step of the repair process is the specific recognition of CPD and (6-4) photoproduct by CPD photolyase [38] and (6-4) photolyase [9], respectively. After photoexcitation of the FADH^- by near-UV/visible light, an electron is transferred to the damaged DNA, leaving the flavin in the neutral semiquinoid form (FADH°). Following bond cleavage of the DNA dimer, the electron is transferred back to FADH° to restore the active state, FADH^- [8]. In the case of the (6-4) photoproduct, it has been proposed that the bound substrate is converted to a four-membered oxetane ring intermediate [30] catalyzed by two conserved histidines in the active site [31].

Crystal structures of CPD photolyase have demonstrated that the FAD cofactor has an unusual U shape, with the isoalloxazine and adenine rings in close proximity (Figure 3.3) [20, 21, 22, 23]. In addition, the DNA dimer is flipped out of the DNA helix and approaches the FAD cofactor [40, 80], but the distance between the DNA substrate and the FAD cofactor is not certain. Theoretical studies [81, 82, 83], with one exception [25], have predicted that the distance between them precludes van der Waals interactions. A long distance between FAD and the DNA substrate was also suggested by analysis of the electric dipole moment [84] and by EPR and ENDOR [85]. The crystal structure of CPD photolyase complexed with a CPD-like DNA lesion [23], however, showed a direct van der Waals contact of 3 to 4 Å between the cofactor and the thymine dimer (Figure 3.3), a finding also supported by a femtosecond fluorescence and absorption spectroscopic study [19]. Resonance Raman spectra have suggested that changes in the hydrogen bonding environment of the FAD cofactor in CPD photolyase after substrate binding [36] give rise to the increased redox potential of the FAD cofactor [86] and stabilize it in the catalytically active FADH^- state in the enzyme, but the precise alterations of the hydrogen bonding environments have not yet been determined. As for (6-4) photolyase, a crystal structure is not yet available. Although the high sequence homology between the two photolyases suggests that the interaction between (6-

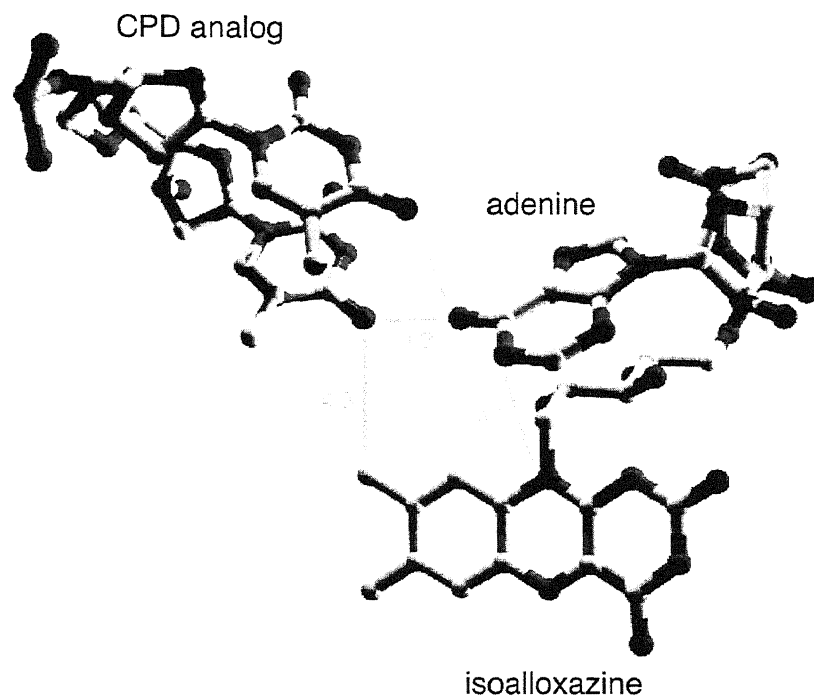


Figure 3.3: Structure of the FAD cofactor and a CPD-like DNA lesion in CPD photolyase (PDB ID: 1TEZ). The distances of possible interactions are given in Å.

4) photoproduct and the FAD cofactor may be similar to that between CPD and FAD in CPD photolyase, the quantum yield for (6-4) photolyase is much lower (0.05-0.1) than that for CPD photolyase (0.7-0.98).

Resonance Raman spectroscopy is a sensitive tool for probing the interactions between the flavin cofactor and its surroundings in flavoproteins [34, 35]. To explore and compare the interactions between the damaged DNA and the FAD cofactor in (6-4) photolyase and CPD photolyase, we first constructed a His-tag expression system to obtain adequate amounts of purified, active enzymes. We then compared the resonance Raman spectra for complexes of the neutral semiquinoid and oxidized forms with damaged DNA. Our results suggest that CPD interacts with both the benzene ring (ring I) and adenine ring of the FAD cofactor, whereas (6-4) photoproduct interacts with only the adenine ring of the FAD cofactor. Such a structural difference may indicate different pathways of electron transfer for the two enzymes. In addition, the Raman spectra predict different substrate-induced changes in the hydrogen bonding environment for the two enzymes.

3.3 Experimental Methods

3.3.1 Enzyme Preparation

The gene of *Arabidopsis thaliana* (6-4) photolyase or *Escherichia coli* CPD photolyase was inserted at the *Nde*I and *Sac*I sites of the pET-28a expression vector (Novagen). *E. coli* BL21(DE3) transformed with the vector was added to 0.5 L of LB medium in a 3-L flask and grown at 37°C to an OD₆₀₀ of 1.5. The culture was then cooled to 26°C, adjusted to 0.2 mM IPTG, incubated for 24 h, and then harvested by centrifugation. The pellet was frozen at -80°C, thawed, resuspended in a lysis buffer (20 mM sodium phosphate, 0.5 M NaCl, 1 mM dithiothreitol [DTT], and 5% glycerol, pH 7.4), and sonicated. Cell debris was removed from the lysate by ultracentrifugation (40000 rpm, 1 h). The cell-free extract was loaded onto a HisTrap HP column (Amersham), and the fusion protein was eluted with elution buffer (20 mM sodium phosphate, 0.5 M NaCl, and 0.5 M imidazole, pH 7.4). Next, the sample was applied to a HiTrap Heparin HP column (Amersham) and eluted with a linear gradient of 0.3 to 1 M NaCl. A 2-L culture of *E. coli* culture yielded approximately 12 mg of (6-4) photolyase and 10 mg of CPD photolyase. The N-terminal His-tag was not removed from the fusion protein.

To prepare the fully oxidized enzyme from the purified sample, (6-4) photolyase was exposed to air for more than 48 h and then applied to a HiLoad 16/60 Superdex 200 prep grade column (Amersham). Because the oxidization of CPD photolyase by air is very ineffective, the neutral semiquinoid FAD cofactor was removed by decreasing the pH, after which CPD photolyase was reconstituted with oxidized FAD (Sigma). All steps were performed according to the procedure described by Jorns et al. [15], except that the DTT was removed from the buffer and a HiTrap phenyl FF (high sub) column (Amersham) was used to remove the excess FAD.

The purified enzyme was stored in 20 mM sodium phosphate (pH 7.4) containing 0.5 M NaCl. Also, 10% glycerol was added to stabilize the reconstituted CPD photolyase. The purity of the protein after the Heparin column was determined by SDS-PAGE, and the monomeric form was identified by gel filtration chromatography on a HiLoad 16/60 Superdex 200 prep grade column. The concentration of the oxidized form of the enzyme was estimated on the basis of the FAD absorbance at 450 nm ($\epsilon_{450} = 1.12 \times 10^4 \text{ M}^{-1}\text{cm}^{-1}$) [43], and that of the neutral semiquinoid form was estimated from the absorbance at 580 nm ($\epsilon_{580} = 4.8 \times 10^3 \text{ M}^{-1}\text{cm}^{-1}$) [44].

3.3.2 Substrate Preparation

The substrate was prepared by irradiation of oligothymine (p(dT)₈ or p(dT)₁₀; Operon) for 30 min with 6.4 mW/cm² of 254 nm UV-light using a UV transilluminator (TFX-20-MC; Vilber Lourmat). The sample was loaded in a cylindrical spinning cell that was cooled during the UV irradiation by flushing with cold N₂ gas passed through liquid N₂. The formation of dimers was monitored by the decrease of the monomer absorption band at 266 nm and the appearance of an absorption band of the (6-4) photoproduct at 325 nm [48].

3.3.3 Enzyme Activity

The enzyme activity of the His-tagged (6-4) and CPD photolyases was measured using a method based on the assay for CPD photolyase [45]. Briefly, the complex of 2 μM photolyase and 50 μM UV-irradiated p(dT)₈ in 50 mM Tris-HCl (pH 7.4), 200 mM NaCl, and 1 mM DTT was placed in a spinning cell and illuminated with a tungsten light (PHL-150; Sigma Koki) at room temperature. The UV-Vis absorption spectrum of the sample was measured as a function of time.

3.3.4 Absorption and Resonance Raman Spectroscopy

Optical absorption spectra of samples were recorded with a Hitachi UV-3310 UV/Vis spectrophotometer at room temperature. Resonance Raman spectra were obtained with a single monochromator (SPEX750M; Jobin Yvon) equipped with a liquid N₂-cooled CCD detector (Spec10:400B/LN; Roper Scientific). The excitation wavelengths were 568.2 and 488.0 nm from a krypton-argon mixed-gas ion laser (BeamLok 2060; Spectra Physics) for the semiquinoid and oxidized forms, respectively. The laser power at the sample point was 5 mW. Rayleigh scattering was removed with appropriate holographic notch filters (Kaiser Optical Systems). Raman shifts were calibrated with indene, and the accuracy of the peak positions of the well-defined Raman bands was ±1 cm⁻¹.

For the semiquinoid form, the measurements were made using an aliquot of 150 μM enzyme in 20 mM sodium phosphate buffer (pH 7.4) containing 0.5 M NaCl. For the oxidized form, the buffer was the same but the enzyme concentration was 75 μM, and 10% glycerol was added for CPD photolyase. A two-fold excess of p(dT)₁₀ or UV-irradiated p(dT)₁₀ was added to the mixture. All measurements were performed with a spinning Raman cell containing 80 μL of sample solution, and all samples were cooled with cold N₂ gas. The structureless background in the raw spectrum was removed by a polynomial subtraction procedure using Igor Pro 5.03 (WaveMetrics). The resonance Raman spectra of oxidized CPD photolyase

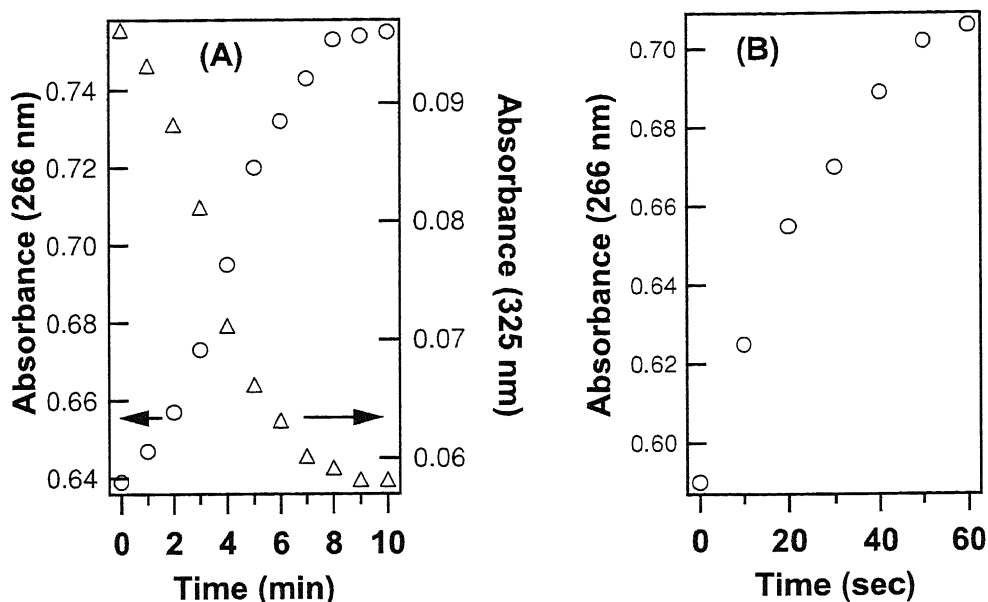


Figure 3.4: Time course of absorption change of UV-damaged p(dT)₈ upon near-UV/visible light irradiation in the presence of (6-4) photolyase (A) and CPD photolyase (B). The absorbance at 266 nm (circles) is due to undamaged DNA, and that at 325 nm (triangles) is due to the (6-4) photoproduct.

were normalized by the Raman band for glycerol in the buffer, so their differences both in frequency and intensity are reliable, whereas all the other Raman data were normalized by their most intense band presumably. Thus, only the differences in frequencies were considered.

3.4 Results

3.4.1 Enzyme Activity

The time course curves for dimer repair by 2 μ M (6-4) photolyase and CPD photolyase in the presence of 50 μ M UV-damaged p(dT)₈ are shown in Figures 3.4A and B, respectively. UV damage substantially reduced the 266-nm band of undamaged DNA and resulted in the appearance of a significant 325-nm band for the (6-4) photoproduct. Illumination of the damaged DNA complex with white light in the presence of (6-4) or CPD photolyases resulted in the gradual reappearance of the 266-nm band and, for the (6-4) photolyase, the disappearance of the 325-nm band. Therefore, although the enzymes used here have N-terminal His-tags, they are catalytically active.

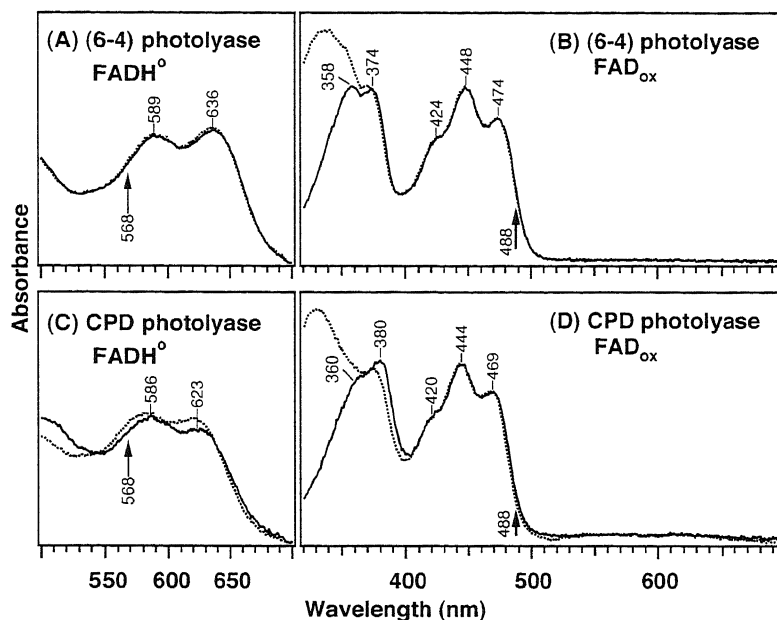


Figure 3.5: Absorption spectra of (6-4) and CPD photolyases in the absence (solid line) and presence (dotted line) of UV-irradiated p(dT)₁₀. (A) Neutral semiquinoid (6-4) photolyase, (B) oxidized (6-4) photolyase, (C) neutral semiquinoid CPD photolyase, (D) oxidized CPD photolyase. The arrows indicate the Raman excitation wavelengths.

3.4.2 Absorption Spectra of Photolyase Complexed with DNA Lesions

Immediately after purification, most of the (6-4) and CPD photolyase was in the neutral semiquinoid form with FADH[•] (Figures 3.5A and C, respectively). The absorption spectra for the fully oxidized (6-4) and CPD photolyases with FAD_{ox} are shown in Figures 3.5B and D, respectively. Also shown are the spectra of the enzyme-substrate complexes with (dotted line) and without substrate (solid line). The absorbance maxima of FADH[•] (586 and 623 nm) and FAD_{ox} (380 nm) in CPD photolyase were significantly shifted upon binding of the UV-damaged DNA.³ This blue shift is in agreement with previous findings [36, 87]. In contrast, substrate binding had little effect on the absorption spectra of (6-4) photolyase.

The absorption maxima around 590 and 630 nm in Figures 3.5A and C are due to the electronic transition of FADH[•]. These absorption maxima are absent from the spectra for FAD_{ox} (Figures 3.5B and D). In accordance with these absorption spectra, we chose 568.2 and 488.0 nm as the Raman excitation wavelengths to se-

³The prominent near-UV absorption maxima around 340 nm shown as a dotted line arises from the UV-damaged DNA of the (6-4) photoproduct [48]. The presence of this band as well as the invariable frequencies of all absorption bands before and after Raman measurement (data not shown) indicate the presence of an adequate amount of UV-damaged DNA substrate in this study.

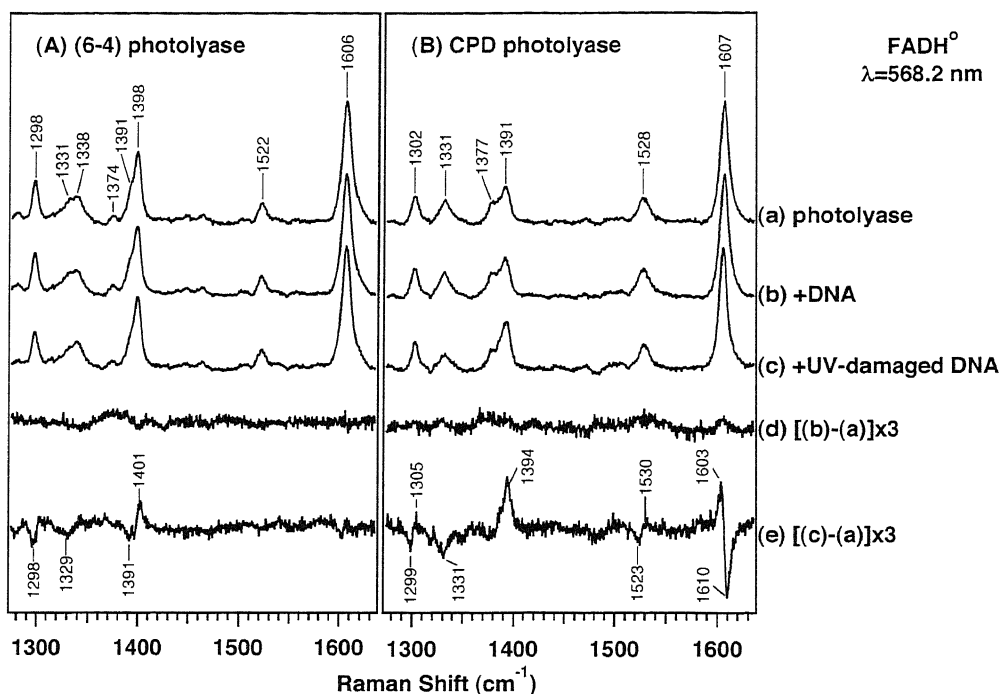


Figure 3.6: Resonance Raman spectra of 150 μM neutral semiquinoid (6-4) photolyase (A) and CPD photolyase (B). In both (A) and (B), subpanel (a) shows the spectrum for enzyme alone, (b) shows the spectrum in the presence of 300 μM p(dT)₁₀, (c) the spectrum in presence of 300 μM UV-irradiated p(dT)₁₀, (d) the difference spectrum [(b) - (a)] \times 3, and (e) the difference spectrum [(c) - (a)] \times 3. The Raman excitation wavelength was 568.2 nm.

lectively enhance the neutral semiquinoid and oxidized forms, respectively (arrows in Figure 3.5).

3.4.3 Resonance Raman Spectra of Neutral Semiquinoid Photolyase Complexed with DNA Lesions

The resonance Raman spectra of the neutral semiquinoid (6-4) photolyase and CPD photolyase are shown in Figures 3.6A and B, respectively. Figure 3.6 shows the spectra for enzyme alone (Figures 3.6A-a and B-a, respectively), with undamaged DNA (Figures 3.6A-b and B-b), and with UV-damaged DNA (Figures 3.6A-c and B-c). Some clear peaks are evident in the difference spectra between enzyme alone and enzyme-UV-irradiated DNA complex (Figures 3.6A-e and B-e) but not in the difference spectra between enzyme alone and enzyme-undamaged DNA complex (Figures 3.6A-d and B-d). These results were repeated in independent experiments, and they suggest that the structure and environment of the FAD cofactor change in both photolyases upon binding of a specific substrate and that undamaged DNA does not interact with the active site in either photolyase. The band near 1606 cm^{-1} in photolyases is a marker for the neutral semiquinoid

FADH ^o in (6-4) Photolyase mode	frequency shift	FADH ^o in CPD Photolyase mode	frequency shift
1606	0	1607	-2
1522	0	1528	+1
1398	+1	1391	+2
1338	0	1331	0
1298	0	1302	+1

Table 3.1: Raman frequency shifts (cm^{-1}) of FADH^o in (6-4) photolyase and CPD photolyase upon substrate binding.

flavin [69]. Recent Raman studies suggested that there are two closely overlapping modes in the frequency region of this marker band and, in fact, splitting of this band can be observed for the D₂O substitution [36, 37]. The higher frequency counterpart arises from the stretching of Ring I, and the lower frequency counterpart comes from C-C/C-N5 stretching and N5-H bending of Ring II (Figure 3.2) [36, 37, 55]. Upon substrate binding to CPD photolyase, there is a significant downshift in the frequency of this marker band. This shift, however, is not detected for the (6-4) photolyase. The 1528 cm^{-1} band of CPD photolyase, which is assigned to the C-C/C-N5 stretching of Ring II and thought to be a sensitive indicator of hydrogen bonding to the N5-H of flavin [37], is upshifted, but this is not observed for (6-4) photolyase. The 1398 cm^{-1} band of (6-4) photolyase and the corresponding band of CPD photolyase at 1391 cm^{-1} , which are tentatively assigned to the C-N10 stretching [37], are both upshifted. The 1338 cm^{-1} band of (6-4) photolyase seems to be unaltered by substrate binding, whereas the bands of the both enzymes at 1331 cm^{-1} seem to be less intensified in the substrate-bound form (Figure 3.6A). The sensitivity of this band to deuterium exchange indicates that it may be influenced by perturbations in the hydrogen bonding environment of the flavin ring [36]. The 1298 and 1302 cm^{-1} bands, which are assigned to C-N5 stretching [37], are upshifted only in CPD photolyase.

These substrate-induced frequency shifts of FADH^o in (6-4) and CPD photolyases are summarized and quantitatively compared in Table 3.1. The frequency changes in CPD photolyase are much larger than those in (6-4) photolyase, and the results are compatible with the changes in the absorption spectra upon substrate binding (Figure 3.5). Notably, the shifts of the Raman bands at 1606 and 1607 cm^{-1} were the most different, indicating different interactions of UV-damaged DNA with FADH^o in the two photolyases.

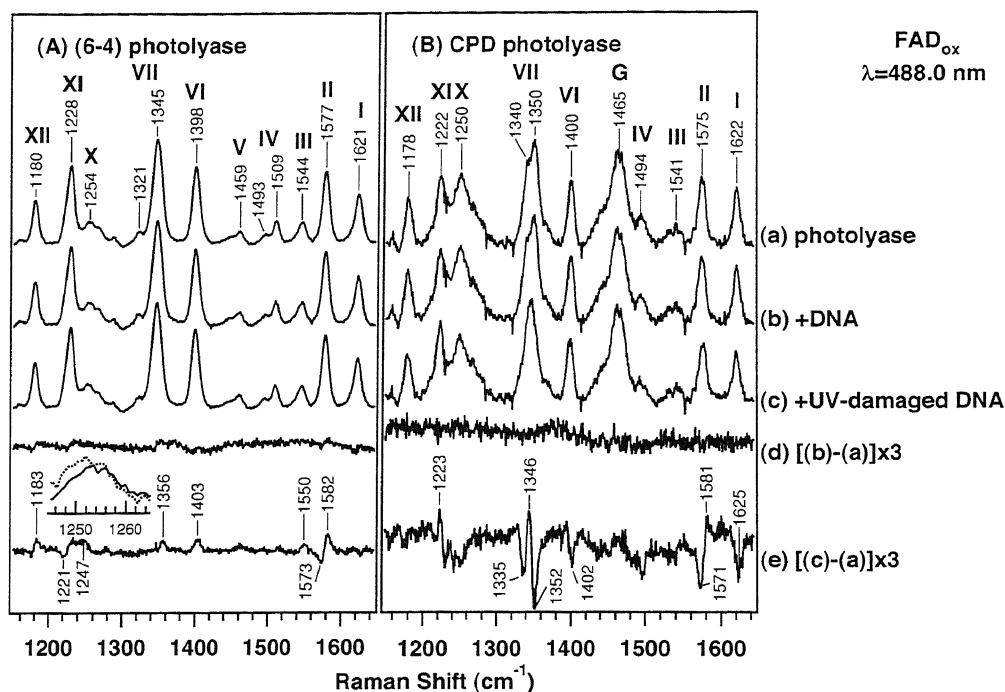


Figure 3.7: Resonance Raman spectra of 75 μM oxidized (6-4) photolyase (A) and CPD photolyase (B). In both (A) and (B), subpanel (a) shows the spectrum for enzyme alone, (b) shows the spectrum in the presence of 150 μM p(dT)₁₀, (c) shows the presence of 150 μM UV-irradiated p(dT)₁₀, (d) the difference spectrum [(b) - (a)] \times 3, and (e) the difference spectrum [(c) - (a)] \times 3. The Raman excitation wavelength was 488.0 nm. G, Raman band of glycerol. Insert: Band X of (6-4) photolyase in the absence (solid line) and presence (dotted line) of UV-irradiated p(dT)₁₀.

3.4.4 Resonance Raman Spectra of Oxidized Photolyase Complexed with DNA Lesions

The vibrational assignments are much better established for the oxidized flavin than for the neutral semiquinoid form [55, 54, 56, 57]. Like the semiquinoid flavin, the oxidized flavin has a planar conformation [88] and should undergo a similar structural change upon substrate binding. Therefore, investigation of the oxidized enzymes could enhance the understanding of the structure and environment of the FAD cofactor in (6-4) and CPD photolyases.

The resonance Raman spectra of the oxidized (6-4) and CPD photolyases are shown in Figures 3.7A and B, respectively. Figure 3.7 shows the spectra for the enzyme alone (Figure 3.7A-a and B-a), with undamaged DNA (Figure 3.7A-b and B-b), and with UV-damaged DNA (Figure 3.7A-c and B-c). The customary numbering of the Raman bands [54] is indicated in the upper part of the figures. Comparison of the difference spectra between the enzyme alone and the enzyme-undamaged DNA complex (Figures 3.7A-d and B-d) and between the enzyme alone

and the enzyme-damaged DNA complex (Figures 3.7A-e and B-e) reveals some peaks that are specifically caused by alterations in the structure and environment of the FAD cofactor upon binding of a damaged DNA substrate. Although the signal-to-noise ratio of the Raman spectra for the reconstituted oxidized CPD photolyase is not as high as that for the oxidized (6-4) photolyase, the frequency shifts observed upon substrate binding are clear and reproducible. The Raman band for glycerol (buffer component), which appears at 1465 cm^{-1} , is indicated by a “G” in Figure 3.7B.

The band I at 1621 or 1622 cm^{-1} was assigned to the almost pure Ring I stretching vibration of the oxidized flavin [55, 54, 56, 57]. Upon substrate binding, a clear downshift of this band was observed only for CPD photolyase. Band II at 1577 or 1575 cm^{-1} was upshifted in both enzymes. Because this band is related to C4a=N5 and N1=C10a stretching, it has been used as a marker of the hydrogen bonding interactions at N1 and N5 of the oxidized flavin [57]. In (6-4) photolyase, the frequency of band III is increased upon substrate binding, whereas those of bands IV and V are not. In contrast, the frequency changes of these weak bands in CPD photolyase cannot be reliably identified. A slight upshift at 1398 cm^{-1} and downshift at 1400 cm^{-1} were observed for band VI in (6-4) photolyase and CPD photolyase, respectively. C-N3 stretching and Ring I modes are believed to contribute to this band [55, 57]. Recent assignments have suggested that the strong band VII is related to the stretching of N10-C10a and N10-C1' (ribityl) [55, 57]. Band VII at 1345 cm^{-1} in (6-4) photolyase was slightly upshifted, whereas in CPD photolyase, it changed from a split peak (1340 and 1350 cm^{-1}) to a single band. Band X at 1254 or 1250 cm^{-1} is another marker band for hydrogen bonding in a flavin moiety. It is thought to reflect the hydrogen bond at N3-H because of its assignment to C-N3 stretching coupled with N3-H bending [55, 57]. This band seems to be downshifted only in (6-4) photolyase. Bands XI (1228 and 1222 cm^{-1}) and XII (1180 and 1178 cm^{-1}) may be related to stretching of C-N3 and Ring I as well as N3-H bending [55, 57]. An increase in frequency was observed for band XI in both enzymes, whereas an increase for band XII was observed in only (6-4) photolyase.

The substrate-induced frequency shifts of FAD_{ox} in (6-4) and CPD photolyases are summarized and quantitatively compared in Table 3.2. The frequency changes in CPD photolyase are much larger than those in (6-4) photolyase and are similar to the results for the neutral semiquinoid enzymes. The substrate-induced downshift in band I and the merge of split band VII in CPD photolyase are the most significant differences with (6-4) photolyase, indicating that the substrate-flavin interactions in CPD photolyase are stronger than in (6-4) photolyase.

band number	FAD _{ox} in (6-4) photolyase mode	FAD _{ox} in (6-4) photolyase frequency shift	FAD _{ox} in CPD photolyase mode	FAD _{ox} in CPD photolyase frequency
I	1621	0	1622	-2
II	1577	+1	1575	+2
VI	1398	<+1	1400	<-1
VII	1345	<+1	1350,1340	-3,+7
X	1254	-1	1250	0
XI	1228	<+1	1222	+1
XII	1180	<+1	1178	0

Table 3.2: Raman frequency shifts (cm^{-1}) of FADH_{ox} in (6-4) photolyase and CPD photolyase upon substrate binding.

3.5 Discussion

3.5.1 Interactions between UV-damaged DNA and the Isoalloxazine Ring of FAD

Figure 3.6 and Table 3.1 show that the marker band of the neutral semiquinoid flavin at 1607 cm^{-1} in CPD photolyase is significantly downshifted upon substrate binding, whereas the corresponding band in (6-4) photolyase is unaltered. This band is thought to be composed of two overlapping modes, namely, vibration of Ring I and the C-C/C-N5/N5-H coupled mode of Ring II. Nishina et al. have reported that this marker band in a neutral semiquinoid riboflavin is insensitive to isotopic substitution of the C and N atoms in Rings II and III of flavin [89], indicating that the vibrations of Ring I are the major contributors to this band. This is also supported by our theoretical assignment of the neutral semiquinoid flavin.⁴ Furthermore, resonance Raman spectra in Figure 3.7 show that band I, which arises from the Ring I stretching of the oxidized flavin, is downshifted only in CPD photolyase upon substrate binding (Table 3.2). Therefore, the alterations of the Ring I vibrations of the isoalloxazine ring cause the significant downshifts of the band at 1607 cm^{-1} of FADH° and 1622 cm^{-1} of FAD_{ox} in CPD photolyase. These Raman spectral features indicate that Ring I of the FAD cofactor interacts with the damaged DNA upon substrate binding in CPD photolyase but not in (6-4) photolyase.

The absorption spectrum of CPD photolyase shows a larger blue shift upon substrate binding than the spectrum for (6-4) photolyase (Figure 3.5). The apparent blue shift of the absorption band at 380 nm for FAD_{ox} in CPD photolyase may indicate a decreased polarity around the isoalloxazine ring because such a

⁴J. Li, T. Uchida, T. Ohta, T. Todo, and T. Kitagawa, *Characteristic Structure and Environment in FAD Cofactor of (6-4) Photolyase along Function Revealed by Resonance Raman Spectroscopy*, *Journal of Physical Chemistry B*, 2006.

shift is also observed for flavin when the solvent is changed from polar to nonpolar [90]. The difference Raman spectrum of FAD_{ox} in CPD photolyase, which was normalized by the solvent band of glycerol, shows a downshift and decrease in intensity of band I as indicated by a negative band at 1625 cm^{-1} in the difference spectrum (Figure 3.7B-e). Such a change in band I in oxidized flavin has been observed when the polarity of its surroundings is reduced [61, 67]. Therefore, the downshifts of the Raman bands at 1607 cm^{-1} of FADH° and 1622 cm^{-1} of FAD_{ox} appear to reflect a decrease in the polarity around the isoalloxazine ring when the pyrimidine bases of CPD approach. Specifically, there is a stronger hydrophobic interaction between CPD and Ring I of isoalloxazine. The hydrophobic interaction has been identified to have the same range as the van der Waals-dispersion force [91]. Therefore, the CPD and Ring I of isoalloxazine in CPD photolyase may make a direct van der Waals contact ($\sim 4\text{ \AA}$), a possibility also suggested by the crystal structure of CPD photolyase containing a substrate analog (Figure 3.3) [23]. MacFarlane and Stanley showed that the electric dipole moment of the CPD is responsible for the electrochromic shift of the electronic transition energy of FAD_{ox} in CPD photolyase, and they estimated a distance of 5.5 to 8 \AA between CPD and FAD [84]. In a later report, they reduced this distance because they observed a very high rate of electron transfer [18]. The absorption spectra upon substrate binding show less of a blue shift in the absorption bands for (6-4) photolyase than for CPD photolyase (Figure 3.5). This smaller change in electronic transition energy induced by damaged DNA indicates a greater distance between the (6-4) photoproduct and the FAD cofactor in (6-4) photolyase. Figure 3.8 shows a schematic illustration of the differences between the positions of DNA lesions and the isoalloxazine ring in the FAD cofactor for the two photolyases.

3.5.2 Interactions between UV-damaged DNA and the Adenine Ring of FAD

Upon substrate binding, the band at 1391 cm^{-1} observed for FADH° in CPD photolyase is upshifted (Figure 3.6). In our previous study, we proposed that this mode is derived mainly from the stretching of the N10-C10a bond in the isoalloxazine ring.³ The X-ray crystal structure of CPD photolyase revealed that the FAD cofactor has a unique U shape, in which an adenine ring approaches to the isoalloxazine ring near the N10-C10a moiety [20, 21, 22, 23]. Therefore, the upshift of the 1391 cm^{-1} band appears to arise from the alteration of the ring stacking conformation between adenine and isoalloxazine rings. Furthermore, the pyrimidine bases of the CPD analog engage in hydrogen bonding interactions with the adenine ring of the FAD cofactor as shown in Figure 3.3. Accordingly, a

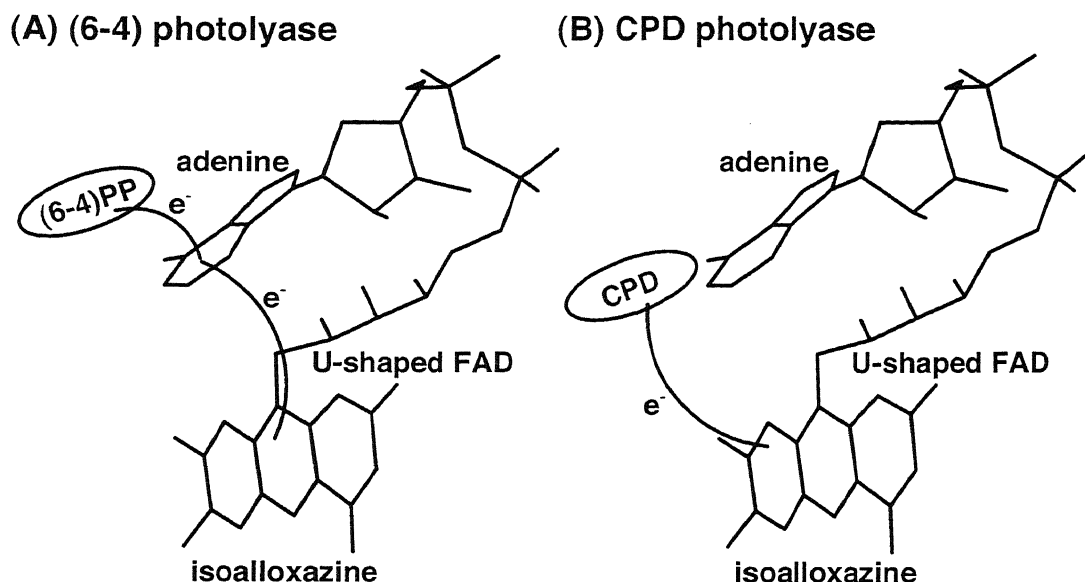


Figure 3.8: Schematic illustration for the positions of a substrate and the putative electron transfer pathways in (6-4) photolyase (A) and CPD photolyase (B). (6-4)PP represents (6-4) photoproduct.

change in ring stacking upon substrate binding is expected due to alterations of the hydrogen bonding interactions between the substrate and the adenine ring of the FAD cofactor, resulting in an upshift of the 1391 cm^{-1} band. The 1398 cm^{-1} band of (6-4) photolyase was also upshifted. Because the FAD binding domains of (6-4) and CPD photolyases are closely related [29], a similar conformational change is also expected to occur in (6-4) photolyase.

Band VII of oxidized flavin, which was assigned to the stretching of N10-C10a and N10-C1' (ribityl), also reflects the vibrations of the N10 atom. Therefore, this mode should also be sensitive to the U-shaped bending and ring stacking conformation of FAD. For (6-4) photolyase, this band is upshifted, and the split band VII in CPD photolyase merged into a single band upon substrate binding (Figure 3.7). These alterations also support the stronger interaction between the adenine ring and UV-damaged DNA (see Figure 3.8).

In (6-4) and CPD photolyases, band II (1577 and 1575 cm^{-1} , respectively) is at a significantly lower frequency than for free FAD (1585 cm^{-1}) [92]. The frequency of band II is known to be downshifted upon formation of a hydrogen bond at N1 of flavin [57]. N1 and the 2'-OH of the ribityl chain are thought to form a strong hydrogen bond because of the U-shape of the FAD cofactor in CPD photolyase [36]. Therefore, the lower frequency of band II in (6-4) and CPD photolyases should reflect a U-shaped conformation of the FAD cofactor. An apparent upshift of band II upon substrate binding is identified for both enzymes (Figure 3.7). This indicates the departure of the adenine ring from the isoalloxazine of FAD as

a result of the hydrogen bonding interaction between adenine and the substrate.

3.5.3 Alterations in Hydrogen Bonding Interactions around FAD Induced by Substrate Binding

The crystal structure of CPD photolyase revealed that N5-H donates a hydrogen bond to an asparagine that is conserved in (6-4) photolyase. Figure 3.6 shows that the Raman band at 1528 cm^{-1} in CPD photolyase is upshifted upon substrate binding, whereas that at 1522 cm^{-1} in (6-4) photolyase is unaltered. This band is a marker for hydrogen bonding at N5-H in neutral semiquinoid flavin [37], and it has been empirically used in a Raman study of P-450 reductase [51]. Therefore, the upshift of the 1522 cm^{-1} band indicates that the hydrogen bond at N5-H of FADH^o in CPD photolyase is weakened when the enzyme is bound to CPD. This Raman prediction is also supported by the more sensitive band at 1302 cm^{-1} in CPD photolyase, which involves C-N5 stretching (Figure 3.6, Table 3.1).

Another hydrogen bonding interaction may be formed at N3-H in both FADH^o and FAD_{ox}. Band X of the oxidized flavin at 1254 cm^{-1} , which reflects C-N3 stretching and N3-H bending, seems to be downshifted in (6-4) photolyase (Figure 3.7 and Table 3.2), indicating that the hydrogen bond would be weakened by substrate binding. The slight frequency shifts of bands VI, XI, and XII in both enzymes (Figure 3.7, Table 3.2) may also reflect the alterations of the hydrogen bonding environment or vibrations of Ring I induced by substrate binding. On the other hand, the Raman bands of FADH^o at 1338 and 1331 cm^{-1} in (6-4) photolyase approach the profile of the single band at 1331 cm^{-1} in CPD photolyase. The lower frequency of band X suggests that the hydrogen bond at N3-H in CPD photolyase is weaker than that in (6-4) photolyase; therefore, the hydrogen bond at N3-H in (6-4) photolyase may be weakened upon substrate binding.

3.5.4 Implication for Biological Functions

Although the crystal structure of CPD photolyase shows that Ring I is in the direction of the DNA lesion [23], previous studies revealed a lower density for unpaired electron and approximately for the whole electrons on the Ring I of semiquinoid flavin radical, suggesting that electron transfer between the isoalloxazine ring and CPD is not direct [24, 73, 2]. It was assumed that the adenine ring of the U-shaped FAD fills the gap between the isoalloxazine ring and damaged DNA and provides effective coupling between them [25]; however, a recent study using femtosecond absorption spectroscopy concluded that there is a direct electron transfer from FAD to CPD because intramolecular electron transfer could not

be observed in the absence of substrate [19]. Our Raman study also suggests that CPD makes a direct contact with Ring I of the isoalloxazine ring within a van der Waals distance and that it interacts with the adenine ring. Therefore, our results support a direct electron transfer from the flavin ring to CPD in CPD photolyase, although modulation of the electron transfer by the adenine ring cannot be ruled out. In contrast, in (6-4) photolyase, the (6-4) photoproduct is located slightly farther from the flavin ring and does not come into contact with it. This indicates that electron transfer in (6-4) photolyase from the flavin ring to the (6-4) photoproduct via the bridged adenine ring is more likely than a direct transfer. The putative electron transfer pathways in (6-4) and CPD photolyase are illustrated in Figure 3.8.

The hydrogen bonding environment is an important factor controlling the redox potential of flavin in flavoproteins [10]. In a study on the control of the redox potential of flavodoxin, introduction of a β -branched threonine side chain at position 57 was shown to change the protein environment of the isoalloxazine ring of FMN, and hydrogen bonding at N5-H of flavin was expected to be weaker than in the native enzyme based on the lower pK_a value of N5-H. This modification of the hydrogen bonding structure of the flavin ring is expected to lead to a significant increase in the redox potential for the semiquinone/hydroquinone couple [76]. Furthermore, molecular orbital calculations showed that the weakened hydrogen bond at donor positions (N3-H and N5-H) would decrease the lowest unoccupied molecular orbital (LUMO) energy [93, 94, 95]. This would enhance the electron acceptability, increasing the redox potential of flavin. In this study, we confirmed that the hydrogen bond at N5-H of FAD in CPD photolyase is weakened upon substrate binding. Therefore, weakening of the hydrogen bond at N5-H by the perturbation of the active site upon binding of CPD is expected to increase the redox potential of the CPD photolyase-substrate complex [86]. In photolyases, $FADH^\circ$ is generated during DNA repair and must be reduced to $FADH^-$ before the next catalytic cycle. Such an increase in the redox potential upon CPD binding is in favor of the reverse electron transfer from the repaired DNA to $FADH^\circ$ as well as the high quantum yield for CPD photolyase. Similarly, a weakened hydrogen bond at N(3)-H in (6-4) photolyase may also decrease the lowest unoccupied molecular orbital energy and facilitate the reduction of $FADH^\circ$.

An active photolyase is in an anionic fully reduced form. However, we have no data on the reduced enzyme, since its complex with the substrate is not so stable that the UV-damaged DNA is easily repaired by the probe light during resonance Raman measurements. Anionic reduced flavin as well as neutral semiquinoid and oxidized flavins are planar [88], and the FAD cofactors in the latter two redox states have been suggested to contact the substrate similarly according to our

Raman spectra. In addition, the flipping of CPD out of the DNA helix into the active site cavity has been revealed to be independent of the redox states of the FAD cofactor by fluorescence study on oxidized and fully reduced CPD photolyase [80]. Therefore, the interactions between substrate and FAD cofactor observed in this work were supposed to occur in the fully reduced enzyme, too.

3.6 Conclusion

In the current study, we reported UV-Vis absorption and resonance Raman spectra of the neutral semiquinoid and oxidized (6-4) and CPD photolyases as well as their changes upon substrate binding. We demonstrated that a direct hydrophobic interaction may occur between CPD and Ring I of the FAD in CPD photolyase but that this does not occur for (6-4) photolyase, indicating that the electron transfer mechanisms in these two enzymes may be different. Another hydrogen bond may be formed between UV-damaged DNA and the adenine ring of FAD in both enzymes upon substrate binding. The substrate may also weaken the hydrogen bond at N5-H in CPD photolyase and at N3-H in (6-4) photolyase. The former change could explain the increased redox potential of FAD recently observed in CPD photolyase. These findings should help establish the structure of the DNA-FAD complex and the mechanism by which substrate binding modulates both enzymes.

Chapter 4

General Conclusion

4.1 Structural Characteristics of Active Site in Photolyases

4.1.1 FAD Cofactor

Resonance Raman spectra revealed that the FAD cofactor in (6-4) photolyase is characterized by an electron localized structure, and binds to the protein in a fairly hydrophobic and strong hydrogen bonding environment, which are similar with those of the FAD cofactor in CPD photolyase. Specially, a stronger H-bond at N5-H and a more typical localized electron density structure were identified for the FAD cofactor in (6-4) photolyase. To improve the understanding of the observed Raman spectra, DFT calculations on the neutral semiquinoid flavin were carried out to provide a normal mode assignment for the first time.

4.1.2 FAD Cofactor upon Substrate Binding

The difference resonance Raman spectra between photolyase and its complex with UV-damaged DNA revealed that, upon substrate binding, UV-damaged DNA contacts the adenine ring of FAD in the both photolyases, whereas it contacts the benzene ring of FAD in CPD photolyase only. Besides, the substrate binding weakens the H-bond at N5-H of FAD in CPD photolyase, while it strengthens the H-bond at N3-H of FAD in (6-4) photolyase.

4.2 Implication for Photo-Repair Mechanism of UV-Damaged DNA

4.2.1 Similar Reaction Mechanisms in (6-4) and CPD Photolyases

Although it is generally assumed that the reaction mechanism of (6-4) photolyase is similar to that of CPD photolyase, the evidence for this is scarce because of the lack of structural investigations of (6-4) photolyase. In this study, a FAD cofactor in (6-4) photolyase with similar electronic structure and protein environment to those in CPD photolyase was revealed. Because FAD is the essential cofactor to catalyze the repairing process of UV-damaged DNA, such similar structure and environment of FAD cofactor experimentally supports the supposed similar reaction mechanisms in the two enzymes.

4.2.2 Quantum Yield

Although the structure and environment of the FAD cofactor are similar, a definitely stronger H-bond at N5-H of FAD was identified in (6-4) photolyase. Such a stronger H-bond can decrease the redox potential of neutral semiquinoid flavin and make it difficult to be reduced to the active fully reduced form again before next repairing cycle. If the electron for the reduction of the flavin radical does not come from the repaired DNA, as that supposed in CPD photolyase, but from another photon of photoreduction reaction, the significantly lower quantum yield of photo-repair in (6-4) photolyase could be explained. In fact, the quantum yield of the photoreduction of the neutral semiquinoid FAD cofactor was very low and similar to that of photo-repair in (6-4) photolyase, which supports our hypothesis.

Furthermore, alterations of H-bonding environment of the FAD cofactor induced by substrate binding in the two photolyases may modulate the quantum yield. In more details, the weakened H-bond at N5-H of FAD in CPD photolyase can raise the redox potential of neutral semiquinoid flavin, facilitate the reduction of this flavin radical by the electron from repaired DNA, and result in the high quantum yield. Similarly, the possibly weakened H-bond at N3-H of FAD in (6-4) photolyase may also decrease the lowest unoccupied molecular orbital energy and facilitate the reduction of the flavin radical.

Although the H-bonding environment may modulate the quantum yields in the two photolyases, the biological significance of a stronger H-bond at N5-H of FAD in (6-4) photolyase is still not clear. One possibility is the H-bonding environment

of FAD evolved to adapt the oxetane intermediate, whose electron acceptability may be different with that of CPD. The detailed electron affinity of FAD and oxetane intermediate needs to be clarified.

4.2.3 Electron Transfer Pathway

The reported crystal structures and the higher conserved sequences of FAD binding sites of those in the DNA photolyase/blue light receptor protein family suggest that a FAD cofactor characterizes as a unique and novel U-shaped conformation in this protein family, which is different with the general "extended" conformation of FAD in other flavoproteins. Some theoretical and experimental studies proposed that the U-shaped FAD (the adenine approaches isoalloxazine) facilitates electron transfer between isoalloxazine and substrate through adenine ring by a superexchange mechanism, although the involvement of adenine during repairing process in CPD photolyase was not observed by a femtosecond spectroscopy.

According to this study, the isoalloxazine ring of FAD in (6-4) photolyase presents an electronic structure with more typically localized electron density, which may benefit the indirect electron transfer (bridged by adenine) between isoalloxazine and UV-damaged DNA in this enzyme. In addition, it has been revealed that (6-4) photoproduct contacts adenine ring only, whereas CPD contacts both adenine and the isoalloxazine rings. Therefore, we suppose that the electron transfer pathway between UV-damaged DNA and FAD cofactor during repairing in (6-4) photolyase is more likely to be bridged by an adenine, while that in CPD photolyase may follow a direct hopping. More direct evidences for the participation of adenine in the electron transfer pathway between (6-4) photoproduct and isoalloxazine need further ultrafast spectroscopic studies.

Bibliography

- [1] T. Lindahl. Instability and decay of the primary structure of DNA. *Nature*, 362(6422):709–715, 1993.
- [2] S. Weber. Light-driven enzymatic catalysis of DNA repair: a review of recent biophysical studies on photolyase. *Biochimica Et Biophysica Acta-Bioenergetics*, 1707(1):1–23, 2005.
- [3] A. Yasui and S. J. McCreedy. Alternative repair pathways for UV-induced DNA damage. *Bioessays*, 20(4):291–297, 1998.
- [4] J. E. Cleaver. Photoreactivation. *DNA Repair*, 2(5):629–638, 2003.
- [5] A. Sancar and C. S. Rupert. Cloning of the Phr gene and amplification of photolyase in escherichia-coli. *Gene*, 4(4):295–308, 1978.
- [6] G. B. Sancar, F. W. Smith, and A. Sancar. Identification and amplification of the e. coli phr gene product. *Nucleic Acids Research*, 11(19):6667–78, 1983.
- [7] A. Sancar, F. W. Smith, and G. B. Sancar. Purification of escherichia-coli DNA photolyase. *Journal of Biological Chemistry*, 259(9):6028–6032, 1984.
- [8] A. Sancar. Structure and function of DNA photolyase and cryptochrome blue-light photoreceptors. *Chemical Reviews*, 103(6):2203–2237, 2003.
- [9] T. Todo, H. Ryo, K. Yamamoto, H. Toh, T. Inui, H. Ayaki, T. Nomura, and M. Ikenaga. Similarity among the drosophila (6-4)photolyase, a human photolyase homolog, and the DNA photolyase-blue-light photoreceptor family. *Science*, 272(5258):109–112, 1996.
- [10] R. Miura. Versatility and specificity in flavoenzymes: Control mechanisms of flavin reactivity. *Chemical Record*, 1(3):183–194, 2001.
- [11] G. Payne, P. F. Heelis, B. R. Rohrs, and A. Sancar. The active form of escherichia coli DNA photolyase contains a fully reduced flavin and not a flavin radical, both in vivo and in vitro. *Biochemistry*, 26(22):7121–7, 1987.

- [12] J. L. Johnson, S. Hamm-Alvarez, G. Payne, G. B. Sancar, K. V. Rajagopalan, and A. Sancar. Identification of the second chromophore of escherichia coli and yeast DNA photolyases as 5,10-methenyltetrahydrofolate. *Proceedings of the National Academy of Sciences of the United States of America*, 85(7):2046–50, 1988.
- [13] T. Ueda, A. Kato, S. Kuramitsu, H. Terasawa, and I. Shimada. Identification and characterization of a second chromophore of DNA photolyase from thermus thermophilus HB27. *Journal of Biological Chemistry*, 280(43):36237–36243, 2005.
- [14] J. E. Hearst. The structure of photolyase - using photon energy for DNA-repair. *Science*, 268(5219):1858–1859, 1995.
- [15] M. S. Jorns, G. B. Sancar, and A. Sancar. Identification of a neutral flavin radical and characterization of a 2nd chromophore in escherichia-coli DNA photolyase. *Biochemistry*, 23(12):2673–2679, 1984.
- [16] Y. F. Li, P. F. Heelis, and A. Sancar. Active-site of DNA photolyase - tryptophan-306 is the intrinsic hydrogen-atom donor essential for flavin radical photoreduction and DNA-repair in vitro. *Biochemistry*, 30(25):6322–6329, 1991.
- [17] M. Byrdin, A. P. M. Eker, M. H. Vos, and K. Brettel. Dissection of the triple tryptophan electron transfer chain in escherichial coli DNA photolyase: Trp382 is the primary donor in photoactivation. *Proceedings of the National Academy of Sciences of the United States of America*, 100(15):8676–8681, 2003.
- [18] A. W. MacFarlane and R. J. Stanley. Cis-syn thymidine dimer repair by DNA photolyase in real time. *Biochemistry*, 42(28):8558–8568, 2003.
- [19] Y. T. Kao, C. Saxena, L. J. Wang, A. Sancar, and D. P. Zhong. Direct observation of thymine dimer repair in DNA by photolyase. *Proceedings of the National Academy of Sciences of the United States of America*, 102(45):16128–16132, 2005.
- [20] H. W. Park, S. T. Kim, A. Sancar, and J. Deisenhofer. Crystal-structure of DNA photolyase from escherichia-coli. *Science*, 268(5219):1866–1872, 1995.
- [21] T. Tamada, K. Kitadokoro, Y. Higuchi, K. Inaka, A. Yasui, P. E. deRuiter, A. P. M. Eker, and K. Miki. Crystal structure of DNA photolyase from anacystis nidulans. *Nature Structural & Molecular Biology*, 4(11):887–891, 1997.

- [22] H. Komori, R. Masui, S. Kuramitsu, S. Yokoyama, T. Shibata, Y. Inoue, and K. Miki. Crystal structure of thermostable DNA photolyase: Pyrimidine-dimer recognition mechanism. *Proceedings of the National Academy of Sciences of the United States of America*, 98(24):13560–13565, 2001.
- [23] A. Mees, T. Klar, P. Gnau, U. Hennecke, A. P. M. Eker, T. Carell, and L. O. Essen. Crystal structure of a photolyase bound to a CPD-like DNA lesion after in situ repair. *Science*, 306(5702):1789–1793, 2004.
- [24] C. W. M. Kay, R. Feicht, K. Schulz, P. Sadewater, A. Sancar, A. Bacher, K. Mobius, G. Richter, and S. Weber. EPR, ENDOR, and TRIPLE resonance spectroscopy on the neutral flavin radical in escherichia coli DNA photolyase. *Biochemistry*, 38(51):16740–16748, 1999.
- [25] J. Antony, D. M. Medvedev, and A. A. Stuchebrukhov. Theoretical study of electron transfer between the photolyase catalytic cofactor FADH(-) and DNA thymine dimer. *Journal of the American Chemical Society*, 122(6):1057–1065, 2000.
- [26] D. Medvedev and A. A. Stuchebrukhov. DNA repair mechanism by photolyase: Electron transfer path from the photolyase catalytic cofactor FADH(-) to DNA thymine dimer. *Journal of Theoretical Biology*, 210(2):237–248, 2001.
- [27] R. Bittl and S. Weber. Transient radical pairs studied by time-resolved EPR. *Biochimica Et Biophysica Acta-Bioenergetics*, 1707(1):117–126, 2005.
- [28] M. K. Cichon, S. Arnold, and T. Carell. A (6-4) photolyase model: Repair of DNA (6-4) lesions requires a reduced and deprotonated flavin. *Angewandte Chemie-International Edition*, 41(5):767–+, 2002.
- [29] T. Todo. Functional diversity of the DNA photolyase blue light receptor family. *Mutation Research-DNA Repair*, 434(2):89–97, 1999.
- [30] S. T. Kim, K. Malhotra, C. A. Smith, J. S. Taylor, and A. Sancar. Characterization of (6-4)-photoproduct DNA photolyase. *Journal of Biological Chemistry*, 269(11):8535–8540, 1994.
- [31] K. Hitomi, H. Nakamura, S. T. Kim, T. Mizukoshi, T. Ishikawa, S. Iwai, and T. Todo. Role of two histidines in the (6-4) photolyase reaction. *Journal of Biological Chemistry*, 276(13):10103–10109, 2001.

- [32] D. S. Hsu, X. D. Zhao, S. Y. Zhao, A. Kazantsev, R. P. Wang, T. Todo, Y. F. Wei, and A. Sancar. Putative human blue-light photoreceptors hCRY1 and hCRY2 are flavoproteins. *Biochemistry*, 35(44):13871–13877, 1996.
- [33] P. J. vanderSpek, K. Kobayashi, D. Bootsma, M. Takao, A. P. M. Eker, and A. Yasui. Cloning, tissue expression, and mapping of a human photolyase homolog with similarity to plant blue-light receptors. *Genomics*, 37(2):177–182, 1996.
- [34] M. D. Morris and R. J. Bienstock. *Advances in Spectroscopy: Spectroscopy of Biological System*, volume 13 of *Spectroscopy of Biological System*. Wiley, New York, 1986.
- [35] J. T. Mcfarland. *Biological Applications of Raman Spectroscopy: Resonance Raman Spectra of Polyenes and Aromatis*, volume 2 of *Resonance Raman Spectra of Polyenes and Aromatis*. Wiley, New York, 1987.
- [36] J. P. M. Schelvis, M. Ramsey, O. Sokolova, C. Tavares, C. Cecala, K. Connell, S. Wagner, and Y. M. Gindt. Resonance Raman and UV-Vis spectroscopic characterization of FADH(center dot) in the complex of photolyase with UV-damaged DNA. *Journal of Physical Chemistry B*, 107(44):12352–12362, 2003.
- [37] D. H. Murgida, E. Schleicher, A. Bacher, G. Richter, and P. Hildebrandt. Resonance Raman spectroscopic study of the neutral flavin radical complex of DNA photolyase from escherichia coli. *Journal of Raman Spectroscopy*, 32(6-7):551–556, 2001.
- [38] A. Sancar. Structure and function of DNA photolyase. *Biochemistry*, 33(1):2–9, 1994.
- [39] T. Todo, H. Takemori, H. Ryo, M. Ihara, T. Matsunaga, O. Nikaido, K. Sato, and T. Nomura. A new photoreactivating enzyme that specifically repairs ultraviolet light-induced (6-4)photoproducts. *Nature*, 361(6410):371–374, 1993.
- [40] X. Zhao, J. Liu, D. S. Hsu, S. Zhao, J. S. Taylor, and A. Sancar. Reaction mechanism of (6-4) photolyase. *Journal of Biological Chemistry*, 272(51):32580–90, 1997.
- [41] A. Sancar. No "end of history" for photolyases. *Science*, 272(5258):48–49, 1996.
- [42] S. Nakajima, M. Sugiyama, S. Iwai, K. Hitomi, E. Otoshi, S. T. Kim, C. Z. Jiang, T. Todo, A. B. Britt, and K. Yamamoto. Cloning and characterization

- of a gene (UVR3) required for photorepair of 6-4 photoproducts in *arabidopsis thaliana*. *Nucleic Acids Research*, 26(2):638-644, 1998.
- [43] T. Todo, S. T. Kim, K. Hitomi, E. Otsoshi, T. Inui, H. Morioka, H. Kobayashi, E. Ohtsuka, H. Toh, and M. Ikenaga. Flavin adenine dinucleotide as a chromophore of the xenopus (6-4)photolyase. *Nucleic Acids Research*, 25(4):764-768, 1997.
- [44] B. Y. Wang and M. S. Jorns. Reconstitution of *escherichia-coli* DNA photolyase with various folate derivatives. *Biochemistry*, 28(3):1148-1152, 1989.
- [45] M. S. Jorns, G. B. Sancar, and A. Sancar. Identification of oligothymidylates as new simple substrates for *escherichia-coli* DNA photolyase and their use in a rapid spectrophotometric enzyme assay. *Biochemistry*, 24(8):1856-1861, 1985.
- [46] A. P. Scott and L. Radom. Harmonic vibrational frequencies: An evaluation of hartree-fock, moller-plesset, quadratic configuration interaction, density functional theory, and semiempirical scale factors. *Journal of Physical Chemistry*, 100(41):16502-16513, 1996.
- [47] M. J. Frisch, G. W. Trucks, H. B. Schlegel, G. E. Scuseria, M. A. Robb, J. R. Cheeseman, Jr. Montgomery, T. J. A.; Vreven, K. N. Kudin, J. C. Burant, J. M. Millam, S. S. Iyengar, V.; Mennucci B.; Cossi M.; Scalmani G.; Rega N.; Petersson G. A.; Nakatsuji H.; Hada M.; Ehara M.; Toyota K.; Fukuda R.; Hasegawa J.; Ishida M.; Nakajima T.; Honda Y.; Kitao O.; Nakai H.; Klene M.; Li X.; Knox J. E.; Hratchian H. P.; Cross J. B.; Bakken V.; Adamo C.; Jaramillo J.; Gomperts R.; Stratmann R. E.; Yazyev O.; Austin A. J.; Cammi R.; Pomelli C.; Ochterski J. W.; Ayala P. Y.; Morokuma K.; Voth G. A.; Salvador P.; Dannenberg J. J.; Zakrzewski V. G.; Dapprich S.; Daniels A. D.; Strain M. C.; Farkas O.; Malick D. K.; Rabuck A. D.; Raghavachari K.; Foresman J. B.; Ortiz J. V.; Cui Q.; Baboul A. G.; Clifford S.; Cioslowski J.; Stefanov B. B.; Liu G.; Liashenko A.; Piskorz P.; Komaromi I.; Martin R. L.; Fox D. J.; Keith T.; Al-Laham M. A.; Peng C. Y.; Nanayakkara A.; Challacombe M.; Gill P. M. W.; Johnson B.; Chen W.; Wong M. W.; Gonzalez C.; Tomasi, J.; Barone, and J. A. Pople. Gaussian 03: Revision C.02. Technical report, Gaussian, Inc., Wallingford CT, 2004.
- [48] W. A. Franklin, K. M. Lo, and W. A. Haseltine. Alkaline lability of fluorescent photoproducts produced in ultraviolet light-irradiated DNA. *Journal of Biological Chemistry*, 257(22):13535-13543, 1982.

- [49] A. Kotaki, M. Naoi, and K. Yagi. Effect of proton donors on absorption spectrum of flavin compounds in apolar media. *Journal of Biochemistry*, 68(3):287-292, 1970.
- [50] Y. Su and G. N. R. Tripathi. Time-resolved resonance Raman observation of protein-free riboflavin semiquinone radicals. *Journal of the American Chemical Society*, 116(10):4405-4407, 1994.
- [51] T. Sugiyama, Y. Nisimoto, H. S. Mason, and T. M. Loehr. Flavins of nadph-cytochrome-P-450 reductase - evidence for structural alteration of flavins in their one-electron-reduced semiquinone states from resonance Raman-spectroscopy. *Biochemistry*, 24(12):3012-3019, 1985.
- [52] T. Kitagawa, H. Sakamoto, T. Sugiyama, and T. Yamano. Formation of the semi-quinone form in the anaerobic reduction of adrenodoxin reductase by nadph - resonance Raman, electron-paramagnetic-res, and optical spectroscopic evidence. *Journal of Biological Chemistry*, 257(20):2075-2080, 1982.
- [53] P. K. Dutta and T. G. Spiro. Resonance coherent anti-stokes Raman-scattering spectra of oxidized and semi-quinone forms of clostridium mp flavodoxin. *Biochemistry*, 19(8):1590-1593, 1980.
- [54] W. D. Bowman and T. G. Spiro. Normal mode analysis of lumiflavin and interpretation of resonance Raman spectra of flavoproteins. *Biochemistry*, 20(11):3313-3318, 1981.
- [55] Y. G. Zheng, J. Dong, B. A. Palfey, and P. R. Carey. Using Raman spectroscopy to monitor the solvent-exposed and "buried" forms of flavin in p-hydroxybenzoate hydroxylase. *Biochemistry*, 38(51):16727-16732, 1999.
- [56] M. Abe and Y. Kyogoku. Vibrational analysis of flavin derivatives - normal coordinate treatments of lumiflavin. *Spectroc. Acta Pt. A-Molec. Biomolec. Spectr.*, 43(8):1027-1037, 1987.
- [57] C. R. Lively and J. T. Mcfarland. Assignment and the effect of hydrogen-bonding on the vibrational normal-modes of flavins and flavoproteins. *Journal of Physical Chemistry*, 94(10):3980-3994, 1990.
- [58] P. K. Dutta, J. R. Nestor, and T. G. Spiro. Resonance coherent anti-stokes Raman-scattering spectra of fluorescent biological chromophores - vibrational evidence for hydrogen-bonding of flavin to glucose oxidase and for rapid solvent exchange. *Proceedings of the National Academy of Sciences of the United States of America*, 74(10):4146-4149, 1977.

- [59] T. Kitagawa, Y. Nishina, Y. Kyogoku, T. Yamano, N. Ohishi, A. Takaisuzuki, and K. Yagi. Resonance Raman-spectra of carbon-13-labeled and nitrogen-15-labeled riboflavin bound to egg-white flavoprotein. *Biochemistry*, 18(9):1804–1808, 1979.
- [60] T. Kitagawa, Y. Fukumori, and T. Yamanaka. Resonance Raman evidence for intramolecular electron-transport from flavin to heme in flavocytochrome-C-552 and nature of chromophoric interactions. *Biochemistry*, 19(25):5721–5729, 1980.
- [61] J. Schmidt, P. Coudron, A. W. Thompson, K. L. Watters, and J. T. Mcfarland. Hydrogen-bonding between flavin and protein - a resonance Raman study. *Biochemistry*, 22(1):76–84, 1983.
- [62] A. J. W. G. Visser, J. Vervoort, D. J. Okane, J. Lee, and L. A. Carreira. Raman-spectra of flavin bound in flavodoxins and in other flavoproteins - evidence for structural variations in the flavin-binding region. *European Journal of Biochemistry*, 131(3):639–645, 1983.
- [63] R. J. Bienstock, L. M. Schopfer, and M. D. Morris. Characterization of the flavin protein-interaction in l-lactate oxidase and old yellow enzyme by resonance inverse Raman-spectroscopy. *Journal of Raman Spectroscopy*, 18(4):241–245, 1987.
- [64] A. Desbois, M. Tegoni, M. Gervais, and M. Lutz. Flavin and heme structures in lactate-cytochrome-c oxidoreductase - a resonance Raman-study. *Biochemistry*, 28(20):8011–8022, 1989.
- [65] M. Tegoni, M. Gervais, and A. Desbois. Resonance Raman study on the oxidized and anionic semiquinone forms of flavocytochrome b(2) and l-lactate monooxygenase. influence of the structure and environment of the isoalloxazine ring on the flavin function. *Biochemistry*, 36(29):8932–8946, 1997.
- [66] T. Picaud and A. Desbois. Electrostatic control of the isoalloxazine environment in the two-electron reduced states of yeast glutathione reductase. *Journal of Biological Chemistry*, 277(35):31715–31721, 2002.
- [67] F. Muller, J. Vervoort, J. Lee, M. Horowitz, and L. A. Carreira. Coherent anti-stokes Raman-spectra of isoalloxazines. *Journal of Raman Spectroscopy*, 14(2):106–117, 1983.
- [68] P. Flukiger, H.P. Luthi, S. Portmann, and J. Weber. MOLEKEL 4.0, Swiss center for scientific computing. Technical report, Manno, Switzerland, 2000.

- [69] Y. Nishina, K. Shiga, K. Horiike, H. Tojo, S. Kasai, K. Matsui, H. Watari, and T. Yamano. Resonance Raman-spectra of semi-quinone forms of flavins bound to riboflavin binding-protein. *Journal of Biochemistry*, 88(2):411–416, 1980.
- [70] M. Sakai and H. Takahashi. One-electron photoreduction of flavin mononucleotide: Time-resolved resonance Raman and absorption study. *Journal of Molecular Structure*, 379:9–18, 1996.
- [71] C. A. Brautigam, B. S. Smith, Z. Q. Ma, M. Palnitkar, D. R. Tomchick, M. Machius, and J. Deisenhofer. Structure of the photolyase-like domain of cryptochrome 1 from *Arabidopsis thaliana*. *Proceedings of the National Academy of Sciences of the United States of America*, 101(33):12142–12147, 2004.
- [72] G. Payne, M. Wills, C. Walsh, and A. Sancar. Reconstitution of *Escherichia coli* photolyase with flavins and flavin analogs. *Biochemistry*, 29(24):5706–5711, 1990.
- [73] S. Weber, K. Mobius, G. Richter, and C. W. M. Kay. The electronic structure of the flavin cofactor in DNA photolyase. *Journal of the American Chemical Society*, 123(16):3790–3798, 2001.
- [74] C. G. Vanschagen and F. Muller. A C-13 NMR-study on free flavins and *Megasphaera elsdenii* and *Azotobacter vinelandii* flavodoxin - C-13-enriched flavins as probes for the study of flavoprotein active-sites. *European Journal of Biochemistry*, 120(1):33–39, 1981.
- [75] Y. Nishina, K. Shiga, K. Horiike, H. Tojo, S. Kasai, K. Yanase, K. Matsui, H. Watari, and T. Yamano. Vibrational-modes of flavin bound to riboflavin binding-protein from egg-white - resonance Raman-spectra of lumiflavin and 8-substituted riboflavin. *Journal of Biochemistry*, 88(2):403–409, 1980.
- [76] M. L. Ludwig, K. A. Pattridge, A. L. Metzger, M. M. Dixon, M. Eren, Y. C. Feng, and R. P. Swenson. Control of oxidation-reduction potentials in flavodoxin from *Clostridium beijerinckii*: The role of conformation changes. *Biochemistry*, 36(6):1259–1280, 1997.
- [77] P. F. Heelis, R. F. Hartman, and S. D. Rose. Photoenzymic repair of UV-damaged DNA - a chemists perspective. *Chemical Society Reviews*, 24(4):289–297, 1995.

- [78] K. Hitomi, S. T. Kim, S. Iwai, N. Harima, E. Otoshi, M. Ikenaga, and T. Todo. Binding and catalytic properties of xenopus (6-4) photolyase. *Journal of Biological Chemistry*, 272(51):32591–32598, 1997.
- [79] G. B. Sancar, M. S. Jorns, G. Payne, D. J. Fluke, C. S. Rupert, and A. Sancar. Action mechanism of escherichia-coli DNA photolyase.3. photolysis of the enzyme-substrate complex and the absolute action spectrum. *Journal of Biological Chemistry*, 262(1):492–498, 1987.
- [80] K. S. Christine, A. W. MacFarlane, K. S. Yang, and R. J. Stanley. Cyclobutylpyrimidine dimer base flipping by DNA photolyase. *Journal of Biological Chemistry*, 277(41):38339–38344, 2002.
- [81] J. Hahn, M. E. Michel-Beyerle, and N. Rosch. Conformation of the flavin adenine dinucleotide cofactor FAD in DNA-photolyase: A molecular dynamics study. *Journal of Molecular Modeling*, 4(2):73–82, 1998.
- [82] D. B. Sanders and O. Wiest. A model for the enzyme-substrate complex of DNA photolyase and photodamaged DNA. *Journal of the American Chemical Society*, 121(22):5127–5134, 1999.
- [83] J. Hahn, M. E. Michel-Beyerle, and N. Rosch. Binding of pyrimidine model dimers to the photolyase enzyme: A molecular dynamics study. *Journal of Physical Chemistry B*, 103(11):2001–2007, 1999.
- [84] A. W. MacFarlane and R. J. Stanley. Evidence of powerful substrate electric fields in DNA photolyase: Implications for thymidine dimer repair. *Biochemistry*, 40(50):15203–15214, 2001.
- [85] S. Weber, G. Richter, E. Schleicher, A. Bacher, K. Mobius, and C. W. M. Kay. Substrate binding to DNA photolyase studied by electron paramagnetic resonance spectroscopy. *Biophysical Journal*, 81(2):1195–1204, 2001.
- [86] Y. M. Gindt, J. P. M. Schelvis, K. L. Thoren, and T. H. Huang. Substrate binding modulates the reduction potential of DNA photolyase. *Journal of the American Chemical Society*, 127(30):10472–10473, 2005.
- [87] M. S. Jorns, B. Y. Wang, S. P. Jordan, and L. P. Chanderkar. Chromophore function and interaction in escherichia-coli DNA photolyase - reconstitution of the apoenzyme with pterin and or flavin derivatives. *Biochemistry*, 29(2):552–561, 1990.

- [88] Y. J. Zheng and R. L. Ornstein. A theoretical study of the structures of flavin in different oxidation and protonation states. *Journal of the American Chemical Society*, 118(39):9402–9408, 1996.
- [89] Y. Nishina, K. Shiga, R. Miura, H. Tojo, M. Ohta, Y. Miyake, T. Yamano, and H. Watari. On the structures of flavoprotein D-amino-acid oxidase purple intermediates - a resonance Raman study. *Journal of Biochemistry*, 94(6):1979–1990, 1983.
- [90] K. Yagi, N. Ohishi, K. Nishimoto, J. D. Choi, and P. S. Song. Effect of hydrogen-bonding on electronic-spectra and reactivity of flavins. *Biochemistry*, 19(8):1553–1557, 1980.
- [91] J. Israelachvili and R. Pashley. The hydrophobic interaction is long-range, decaying exponentially with distance. *Nature*, 300(5890):341–342, 1982.
- [92] M. Benecky, T. Y. Li, J. Schmidt, F. Frerman, K. L. Watters, and J. Mcfarland. Resonance Raman study of flavins and the flavoprotein fatty acyl coenzyme-a dehydrogenase. *Biochemistry*, 18(16):3471–3476, 1979.
- [93] K. Nishimoto, H. Fukunaga, and K. Yagi. Studies in a model system on the effect of hydrogen-bonding at hetero atoms of oxidized flavin on its electron acceptability. *Journal of Biochemistry*, 100(6):1647–1653, 1986.
- [94] K. Nishimoto, E. Kai, and K. Yagi. Hydrogen-bonding of flavoprotein.2. effect of hydrogen-bonding at hetero atoms of reduced flavin on its reactivity. *Biochimica et Biophysica Acta*, 802(2):321–325, 1984.
- [95] K. Yagi. Hydrogen-bonding in flavoproteins. *Chemica Scripta*, 27A:27–30, 1987.

Appendix A

Supplementary Raman Spectra of CPD Photolyase

A.1 CPD Photolyase in D₂O

In Chapter 2, the structure and environment of the FAD cofactor in (6-4) photolyase was investigated by resonance Raman spectroscopy. As for neutral semiquinoid flavin, generally hydrogen atoms at N3 and N5 are exchangeable in D₂O. Unexpectedly, a complete deuterated FAD in (6-4) photolyase, whose N5-D form can be identified by resonance Raman spectra, was only prepared by fully oxidization and subsequent photoreduction in D₂O, but not by buffer exchange. Because the reported resonance Raman spectra of the deuterated FAD in CPD photolyase is very similar to that of the incompletely deuterated CPD in (6-4) photolyase, the H-D exchange of N5-H of FAD in CPD photolyase was believed to be incomplete after buffer exchange. To confirm such a suppose, the *E. coli* CPD photolyase, prepared by experimental methods in section 3, was investigated by resonance Raman spectroscopy in D₂O as shown in Figure A.1. Clearly, the positive peaks at 1595 and 1614 cm⁻¹ in spectrum (c) revealed that the marker band of semiquinoid flavin at 1607 cm⁻¹ split along the Raman measurement in D₂O. Such a split was observed for the neutral semiquinoid FAD in (6-4) photolyase because the oxidized FAD in the sample (a mixture of semiquinoid and oxidized forms) was photoreduced by probing light during measurement (see Chapter 2). Therefore, the split of the 1607 cm⁻¹ band, which gets arise from the N5-D form of FAD in CPD photolyase, was also identified to be caused by light irradiation but not buffer exchange. Accordingly, the deuteration of N5-H at the FAD cofactor in CPD photolyase does not occur in D₂O after buffer exchange like that in (6-4) photolyase.

Besides, a 1522 cm⁻¹ band was identified as a marker band of H-bond at N5-H

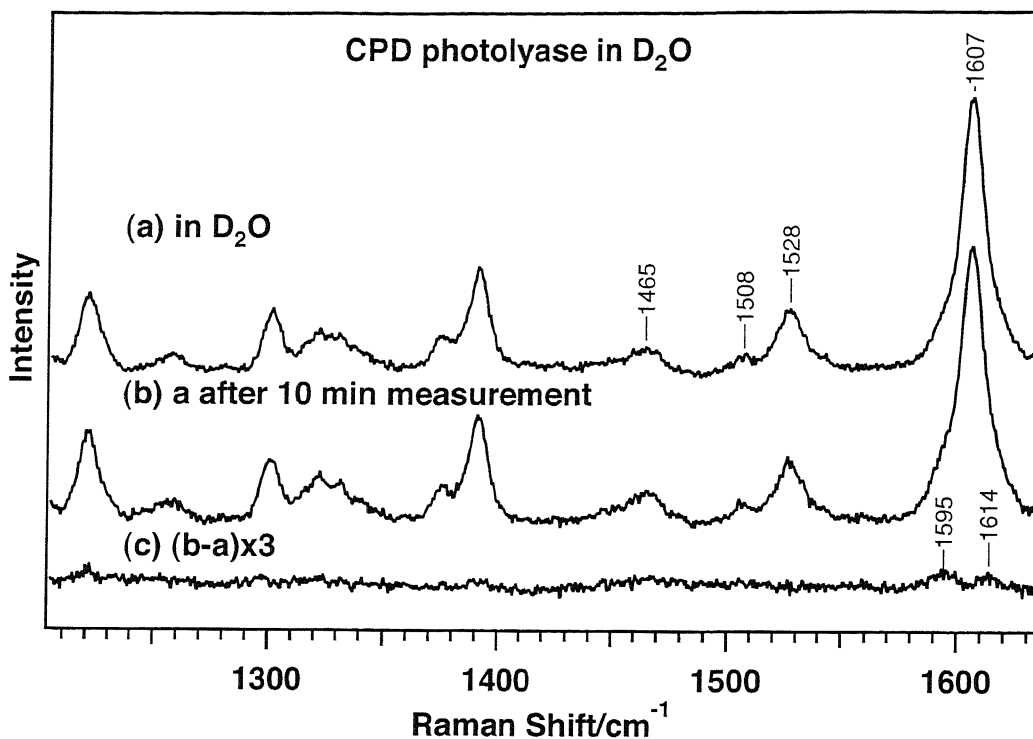


Figure A.1: Resonance Raman spectra of *E. coli* CPD photolyase in a semiquinoid form in D₂O (a), after 10 min repeated measurement in D₂O (b), and their difference spectrum (c). The Raman excitation wavelength was 568.2 nm.

of a neutral semiquinoid FAD because it contains N5-H bending. The frequency of this band in (6-4) photolyase is lower by 6-7 cm⁻¹ than that in CPD photolyase, indicating a stronger H-bond at N5-H of FAD in (6-4) photolyase. A Raman band at 1456 cm⁻¹ was observed for the first time of deuterated neutral semiquinoid FAD in (6-4) photolyase, and was assigned to the N5-H bending component of the 1522 cm⁻¹ band. Therefore, the 1456 cm⁻¹ band should be a more sensitive marker band of H-bond at N5-H of neutral semiquinoid flavin. Figure A.1 showed that the corresponding band in CPD photolyase is at 1465 cm⁻¹, which is 9 cm⁻¹ higher than that in (6-4) photolyase, indicating a weaker H-bond at N5-H of FAD in CPD photolyase. These Raman data support the conclusions in Chapter 2.

A.2 E109A Mutant without MTHF

A H-D sensitive 1378 cm⁻¹ shoulder band in semiquinoid CPD photolyase was supposed to get arise from MTHF, the second chromophore of this enzyme, because it was not observed in a E109A mutant of *E. coli* CPD photolyase whose MTHF is lost. Detailedly, this band was suggested to come from MTHF itself or FAD cofactor stabilized by MTHF. In our study, the same band was also observed in a MTHF lacking (6-4) photolyase, which indicated that this band is not from

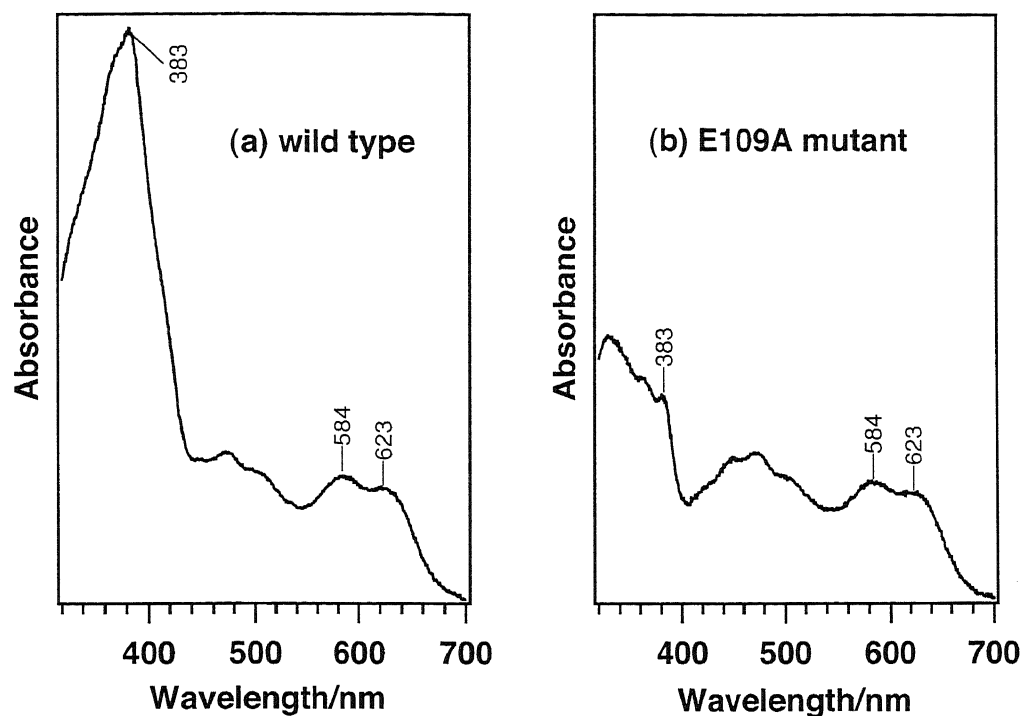


Figure A.2: Absorption spectra of *E. coli* CPD photolyase in wide type (a) and E109A mutant (b).

MTHF itself. In addition, we prepared an E109A mutant and compared it with the wild type. Figure A.2 showed an absorption spectrum of the mutant protein. The 383 nm peak, which is the absorption maximum of MTHF, is almost lost in the E109A mutant. However, the bands at 1378 cm^{-1} in H_2O and 1375 cm^{-1} in D_2O were observed in both the wide type and mutant proteins as shown in Figure A.3. Since our Raman spectra of the E109A mutant have an improved quality compared to the reported one, we conclude that the 1378 cm^{-1} band in CPD photolyase has no relationship with MTHF.

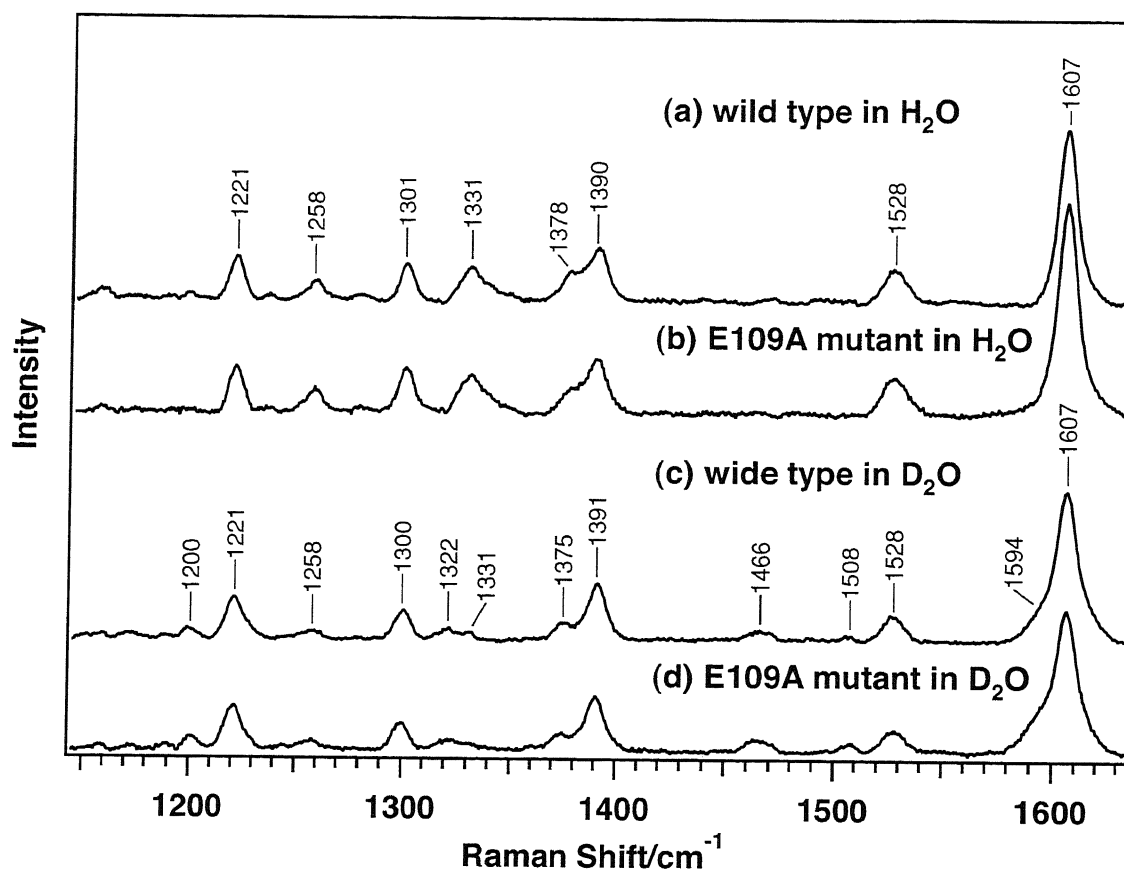


Figure A.3: Resonance Raman spectra of *E. coli* CPD photolyase in a semiquinoid form as (a) wild type in H₂O, (b) E109A in H₂O, (c) wild type in D₂O, (d), E109A in D₂O. The Raman excitation wavelength was 568.2 nm.

Appendix B

Cartesian Coordinates for Optimized Lumiflavin

B.1 Neutral Semiquinoid Lumiflavin

(atom X Y Z):

```
C -3.79315700 -0.64850900 0.00008900
C -1.46448900 -0.63417700 -0.00002000
C -1.40817400 0.78368900 -0.00001900
C -2.62809300 1.56491100 -0.00005200
C 0.98842900 0.79437100 -0.00000800
C 0.97443900 -0.62259300 -0.00000900
C 2.20970200 -1.28286400 -0.00000400
H 2.23417100 -2.36584400 -0.00000400
C 3.42487500 -0.59131700 0.00000200
C 3.42458900 0.82252500 0.00000300
C 2.20226800 1.48915000 -0.00000200
H 2.17745300 2.57646900 -0.00000200
C -0.25308400 -2.77659900 0.00000900
H 0.25353200 -3.15885500 0.89297400
H -1.29254700 -3.09803400 0.00000800
H 0.25353900 -3.15888000 -0.89294200
C 4.72232400 -1.36264200 0.00000800
H 4.54264200 -2.44158600 0.00000600
H 5.33389300 -1.12641000 -0.88038000
H 5.33387800 -1.12642200 0.88040900
C 4.71539400 1.60439500 0.00000900
H 5.32862100 1.37411900 0.88062000
```

```

H 5.32862600 1.37412600 -0.88060000
H 4.52520200 2.68162100 0.00000900
O -4.87864500 -1.20351700 -0.00003600
N -0.24647400 -1.31522500 -0.00002100
N -0.22367200 1.45398500 -0.00001400
N -2.58537900 -1.31901800 0.00000300
N -3.75635100 0.77425900 0.00002500
H -4.65707800 1.23897400 0.00000800
O -2.63092000 2.79877500 0.00002600
H -0.29243500 2.46862300 -0.00001400

```

B.2 Neutral Semiquinoid Lumiflavin with N3-D

(atom X Y Z):

```

C -3.79315700 -0.64850900 0.00008900
C -1.46448900 -0.63417700 -0.00002000
C -1.40817400 0.78368900 -0.00001900
C -2.62809300 1.56491100 -0.00005200
C 0.98842900 0.79437100 -0.00000800
C 0.97443900 -0.62259300 -0.00000900
C 2.20970200 -1.28286400 -0.00000300
H 2.23417100 -2.36584400 -0.00000400
C 3.42487500 -0.59131700 0.00000200
C 3.42458900 0.82252500 0.00000300
C 2.20226800 1.48915000 -0.00000200
H 2.17745300 2.57646900 -0.00000200
C -0.25308400 -2.77659900 0.00000800
H 0.25353200 -3.15885600 0.89297300
H -1.29254700 -3.09803400 0.00000700
H 0.25353900 -3.15888000 -0.89294300
C 4.72232400 -1.36264200 0.00000800
H 4.54264200 -2.44158600 0.00000700
H 5.33389300 -1.12641000 -0.88038000
H 5.33387800 -1.12642200 0.88040900
C 4.71539400 1.60439500 0.00000900
H 5.32862100 1.37411900 0.88062100
H 5.32862600 1.37412600 -\appendix
\setcounter{chapter}{0}\renewcommand{\chaptername}{Appendix}0.88059900
H 4.52520200 2.68162100 0.00000900

```

O -4.87864500 -1.20351700 -0.00003600
N -0.24647400 -1.31522500 -0.00002100
N -0.22367200 1.45398500 -0.00001400
N -2.58537900 -1.31901800 0.00000300
N -3.75635100 0.77425900 0.00002500
H -4.65707800 1.23897400 0.00000900
O -2.63092000 2.79877500 0.00002600
H -0.29243500 2.46862300 -0.00001400

B.3 Neutral Semiquinoid Lumiflavin with N3-D, N5-D

(atom X Y Z):

C -3.79315700 -0.64850900 0.00008900
C -1.46448900 -0.63417700 -0.00002000
C -1.40817400 0.78368900 -0.00001900
C -2.62809300 1.56491100 -0.00005200
C 0.98842900 0.79437100 -0.00000800
C 0.97443900 -0.62259300 -0.00000900
C 2.20970200 -1.28286400 -0.00000300
H 2.23417100 -2.36584400 -0.00000400
C 3.42487500 -0.59131700 0.00000200
C 3.42458900 0.82252500 0.00000300
C 2.20226800 1.48915000 -0.00000200
H 2.17745300 2.57646900 -0.00000200
C -0.25308400 -2.77659900 0.00000800
H 0.25353200 -3.15885600 0.89297300
H -1.29254700 -3.09803400 0.00000700
H 0.25353900 -3.15888000 -0.89294300
C 4.72232400 -1.36264200 0.00000800
H 4.54264200 -2.44158600 0.00000700
H 5.33389300 -1.12641000 -0.88038000
H 5.33387800 -1.12642200 0.88040900
C 4.71539400 1.60439500 0.00000900
H 5.32862100 1.37411900 0.88062100
H 5.32862600 1.37412600 -0.88059900
H 4.52520200 2.68162100 0.00000900
O -4.87864500 -1.20351700 -0.00003600

N -0.24647400 -1.31522500 -0.00002100
N -0.22367200 1.45398500 -0.00001400
N -2.58537900 -1.31901800 0.00000300
N -3.75635100 0.77425900 0.00002500
H -4.65707800 1.23897400 0.00000900
O -2.63092000 2.79877500 0.00002600
H -0.29243500 2.46862300 -0.00001400